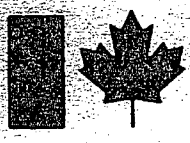

Environment Canada

Environnement Canada

Canada Centre For Inland Waters

Centre Canadien Des Eaux Intérieures

VAPS

PRELIMINARY SYSTEM DATA EVALUATIONS

ENGINEERING SERVICES SECTION

ES-513

UNPUBLISHED REPORT
RAPPORT NON PUBLIÉ

VAPS
PRELIMINARY SYSTEM DATA EVALUATIONS

ENGINEERING SERVICES SECTION

ES-513

by

P. F. Hamblin
W. H. Gibson
L. R. Muir

SSD/CCIW/IWD

March, 1977

ACKNOWLEDGEMENTS

The authors gratefully acknowledge the assistance of the following CCIW groups:-

- Electronics Engineering Unit for advice, design troubleshooting of winch control and data acquisition packages.
- Technical Operations Section for field deployment and retrieval.
- Data Management Service for extraction, manipulation and plotting of data.

ABSTRACT

This report is an engineering and scientific evaluation of an instrumentation package known as the Vertical Automated Profiling System which measures, in an unattended self-recording mode, such physical variables as temperature, time depth, current direction and speed, and engineering data such as instrument tilt.

First, a brief description is provided, followed by the results of three experimental tests: 1) the towing tank tests, 2) the field dwell experiments, and 3) the field profiling runs. Finally, evaluations and recommendations are summarized. In an appendix, the calibration curves and conversion relations are tabulated for the various sensors.

TABLE OF CONTENTS

LIST OF TABLES AND FIGURES

Tow Tank Drag Tests

There were two sets of tow tank drag tests conducted at different times. The first test was conducted, prior to any field tests, for the calibration of the sensors. The second test was conducted after the field test to confirm that certain motions of the vehicle, which were deduced from the analysis of the field data, were actually occurring.

1.1 First Tow Tank Drag Test

The sensor vehicle was rigged as in figure 1 for towing in the Hydraulics tow tank at various constant speeds. The tow tank is 100 metres long by 3 metres deep. The vehicle was towed at 2, 5, 10, 15, 20, 30, and 100 cm/sec, and each individual speed was held constant for at least 5 minutes, except for the 100 cm/sec case where the speed was held constant for as long as possible.

There were visible trailing eddies at the surface of the buoyancy tanks, due to rough edges and weld protrusions, at all speeds, and these increased in length and width as the towing speed increased. Above 10 cm/sec, the vehicle adopted a simultaneous translating and rotating motion, and at 30 cm/sec the period of this motion was approximately 15 seconds. The amplitude of the yawing motion was approximately 50 cm, and the amplitude of the rotation was about 45°. With increased towing speeds, the vehicle tilted downstream more and more.

The statistics of the 7 runs at speeds between zero and 30 cm/sec are summarized in Table 1 in the form of means and standard deviations and in figures 2 to 6. In figure 1, the error bars represent the standard deviations, and in figures 2 to 5 the error bars represent the 95% confidence intervals for estimation of the means.

In the case of mean depth, the slight increase of 6 cm over the entire range is thought to be due to the tilt of the vehicle with increased towing speed. The uncertainty in the resolution of depth is not strongly affected by carriage speed and is estimated to be about ±20 cm.

The error in the mean speed is largest at low towing speed and attains a value of 37% overestimation at 2 cm/sec. At higher speeds the errors are less than 10% and do not appear to have a systematic variation with speed. It should be noted that at speeds higher than 10 cm/sec,

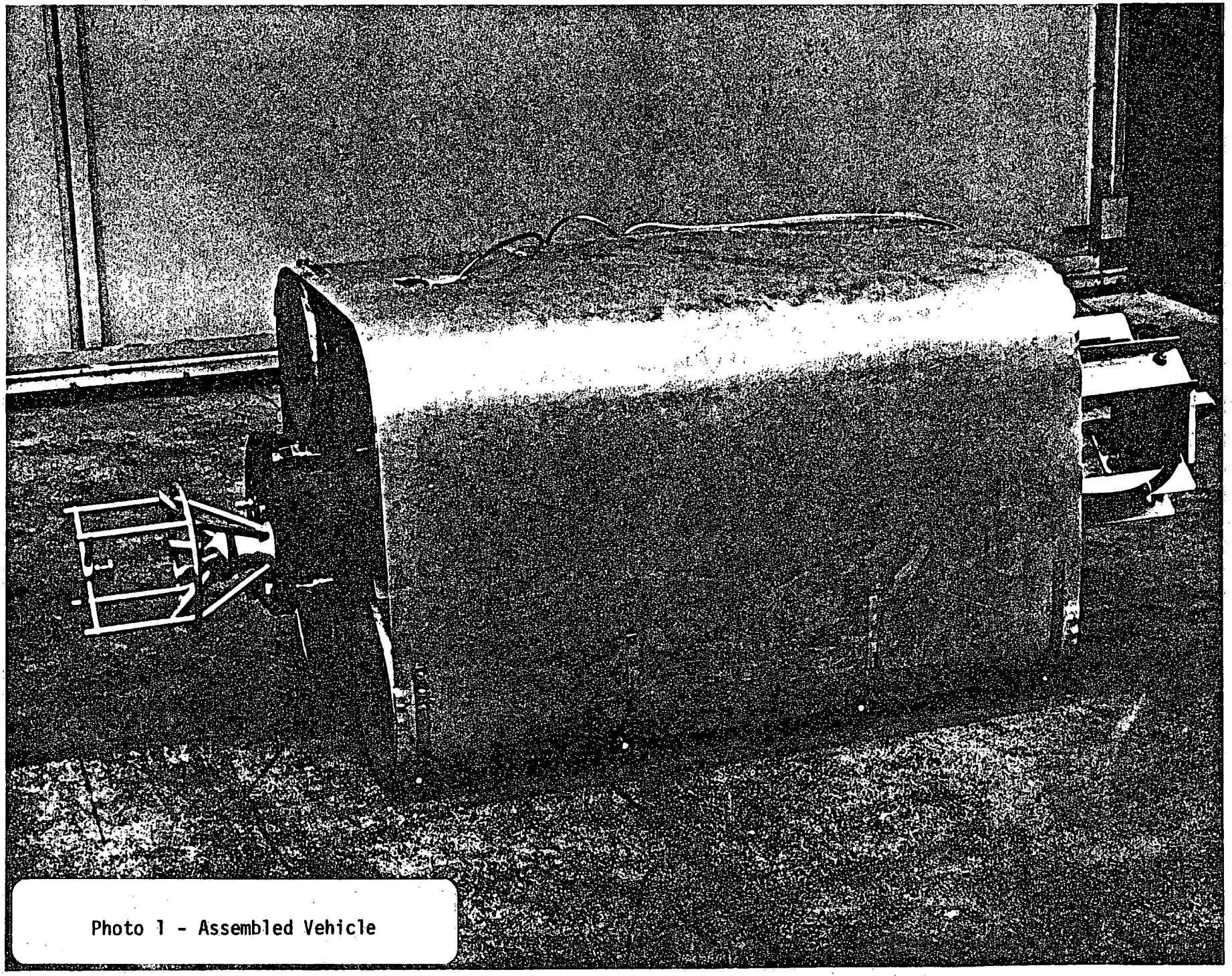

Photo 1 - Assembled Vehicle

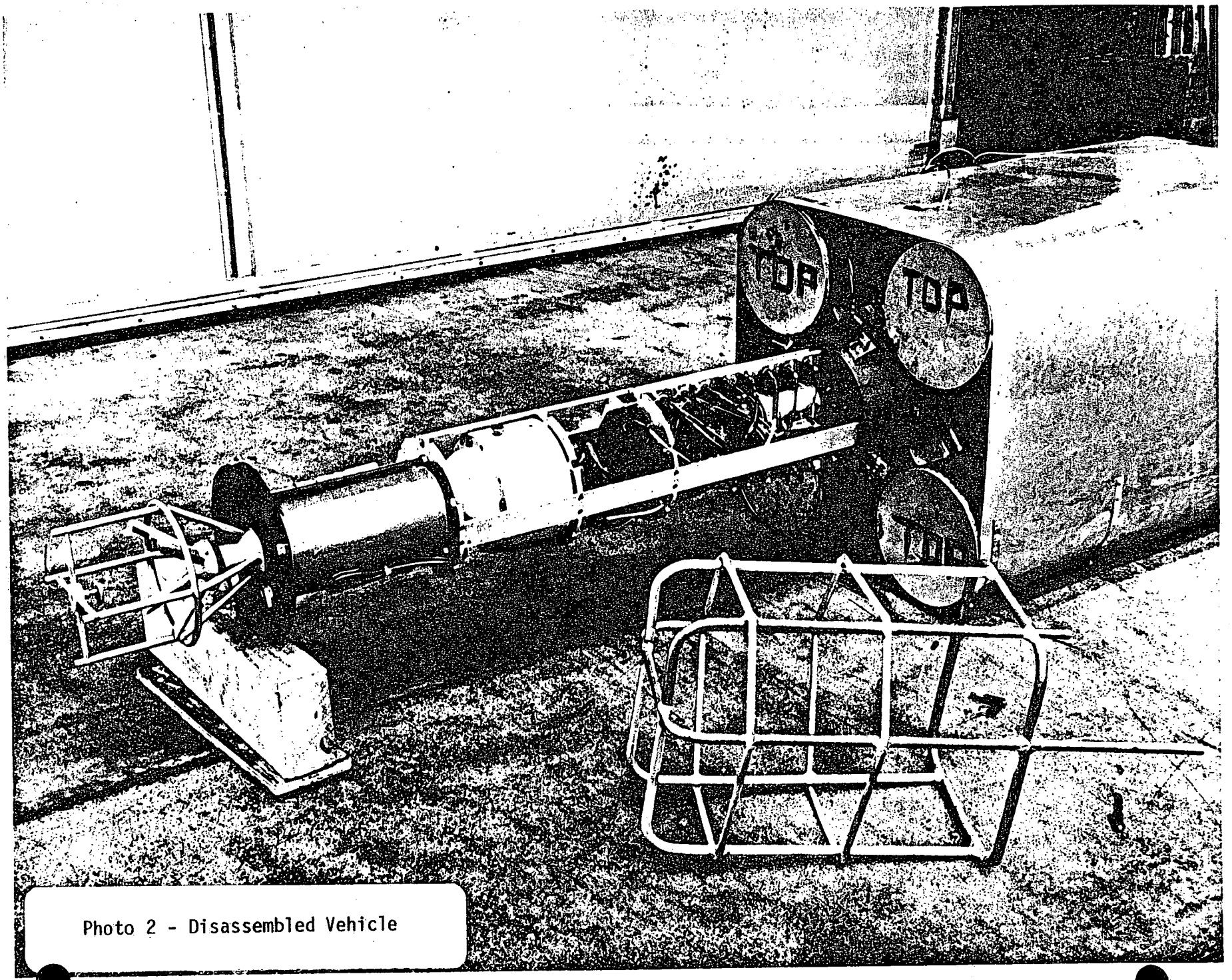

Photo 2 - Disassembled Vehicle

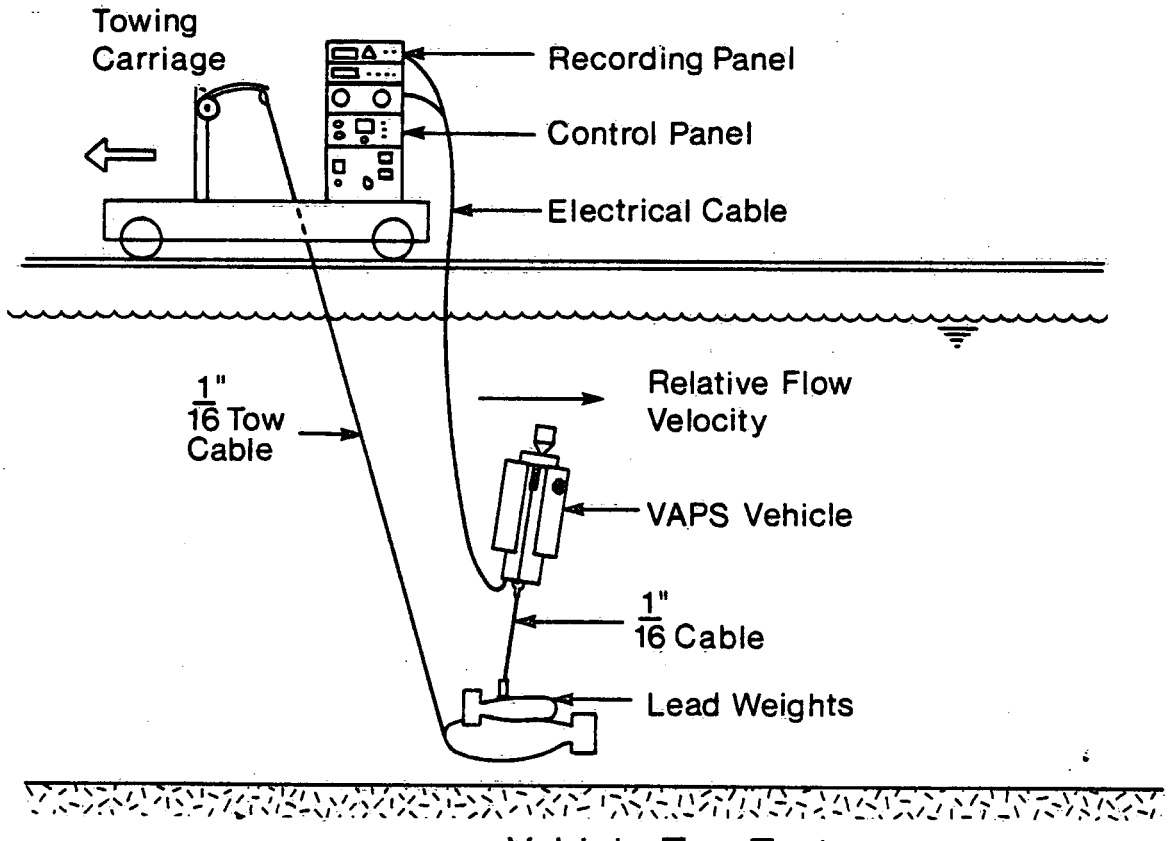

Figure 1. Tow Tank Test Number 1. Rigging of Complete Vaps on Towing Carriage

oscillation in the vehicle motion probably contributed to the overall mean speed.

Because of the vertical motion of the vehicle in the actual field configuration of the profiler, it would have been desirable to test the off-axis response of the current meter. Unfortunately, time did not permit this test to be conducted.

Considering the fact that there were probably many disturbing influences in the magnetic field in the towing tank, there is remarkably little variation in the mean compass readings from run to run. The mean angle is an arithmetic mean, not a vector mean, which is thought to be justified for small deviations from the mean. The large error bands at higher speeds reflect the oscillation of the vehicle about the vertical axis and not increased uncertainty in the compass readings.

The computed direction of the current involved calculation of the direction relative to the instrument axes plus the direction of these axes from magnetic north. Because of the disturbing influences of the magnetic field in the test facility, it is difficult to say more than that there is generally acceptable qualitative agreement of the current direction with the east-west alignment of the towing tank. In the runs at 15 and 30 cm/sec, the carriage advanced to the west implying a current of 90°.

The mean tilt angle increases up to 3° at 30 cm/sec which correlated with the slight increase in depth (figure 2). Larger error bars probably indicate an instability of the vehicle at higher towing speeds.

It is expected that the direction of tilt should correlate directly with the direction of current. In figure 6, the difference between the mean tilt angle and the current direction is considerable (60°) at low towing speeds but approaches much smaller angles at higher towing speeds. Either there is a systematic offset error in the tilt sensor or the instrument does not align itself in the vertical direction at the equilibrium position.

1.2 Second Tow Tank Drag Test

The second tow tank drag test was conducted to verify some conclusions that had been drawn from the analysis of the field data. The

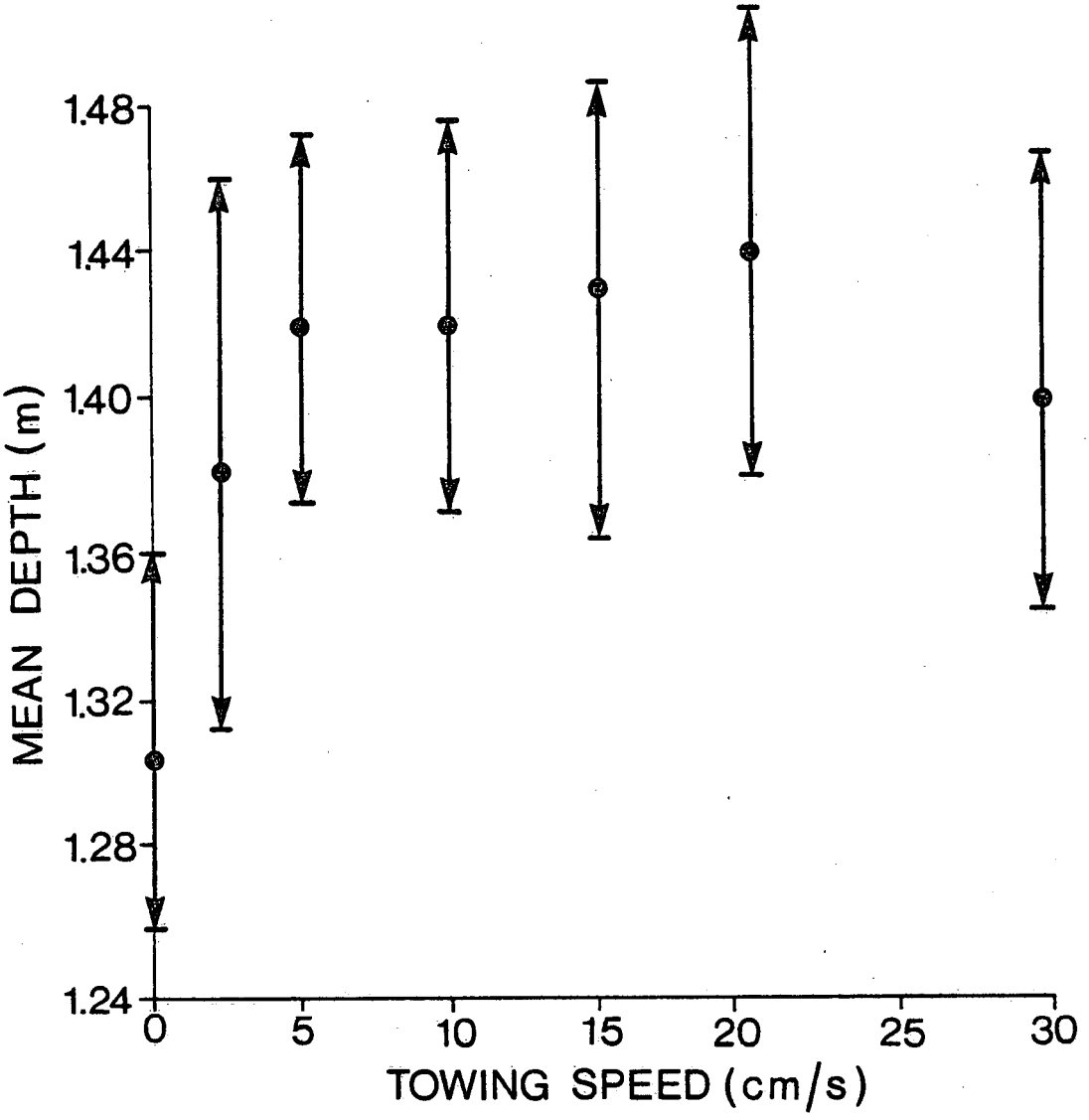
1.48
1.44
1.40
1.36
1.32
1.28
1.24
MEAN DEPTH (m)
0
5
10
15
20
25
30
TOWING SPEED (cm/s)

FIGURE 2.

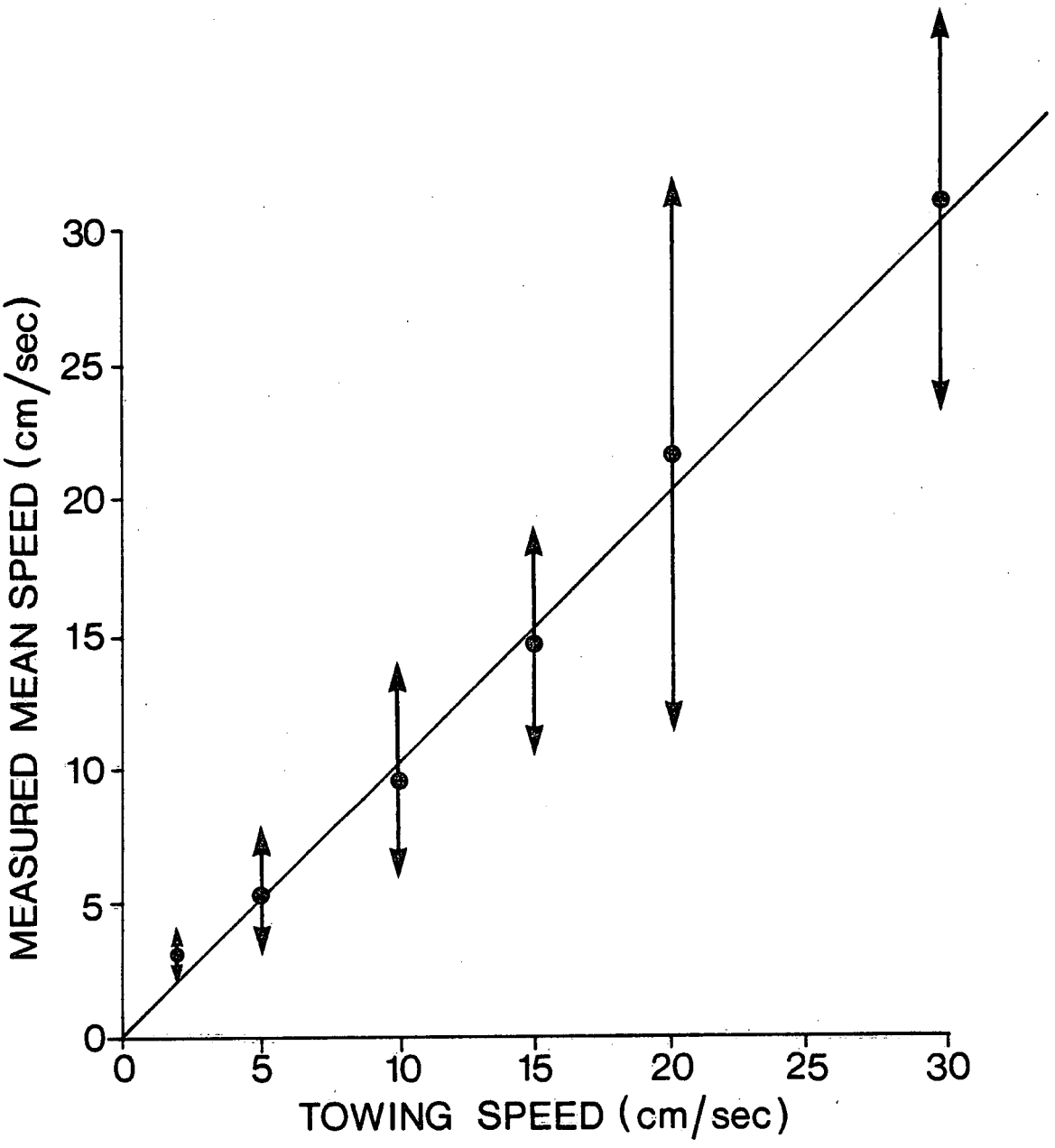
MEASURED MEAN SPEED (cm/sec)
30
25
20
15
10
5
0
0
5
10
15
20
25
30
TOWING SPEED (cm/sec)

FIGURE 3

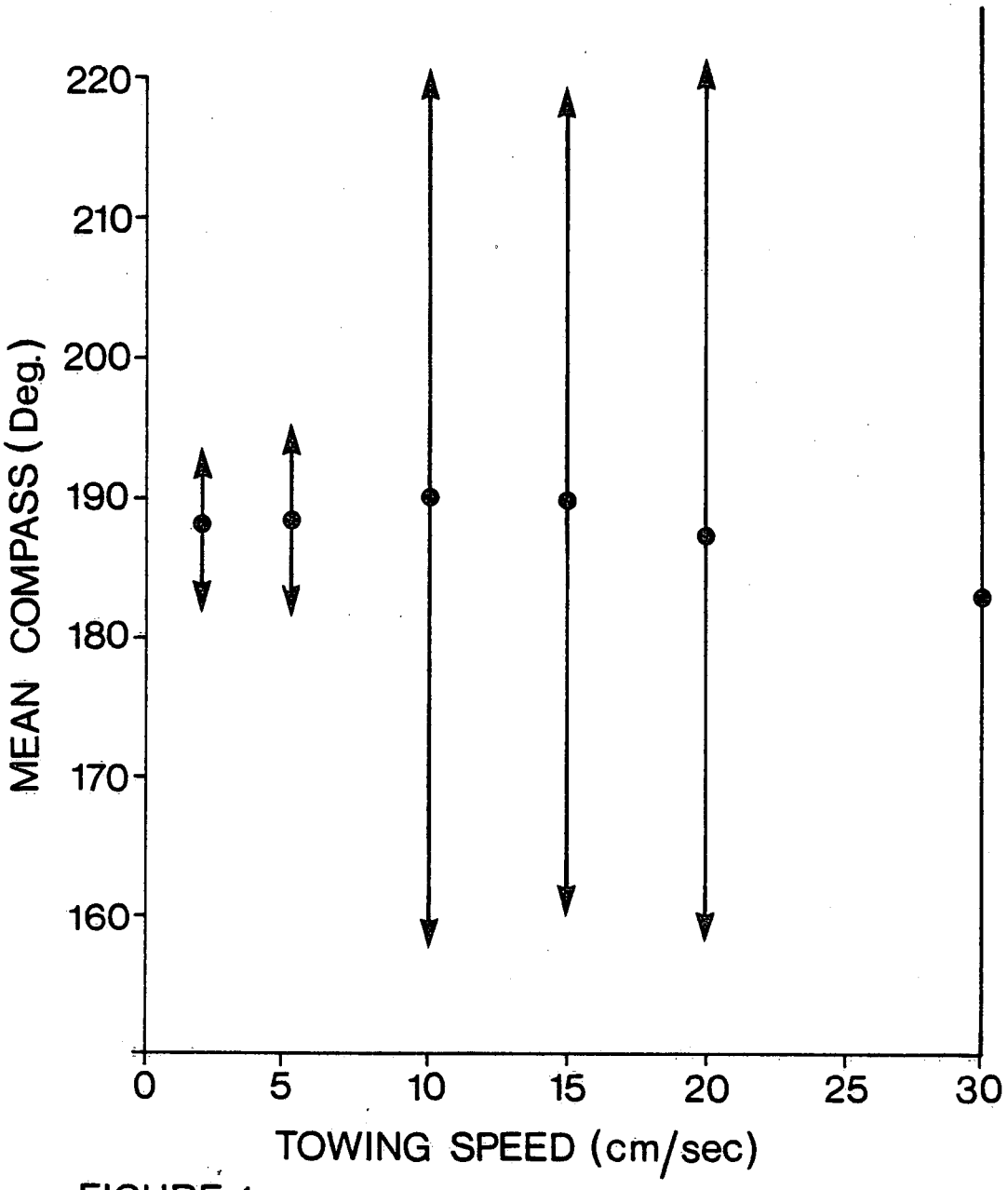
220
210
200
190
180
170
160
MEAN COMPASS (Deg.)
0
5
10
15
20
25
30
TOWING SPEED (cm/sec)

FIGURE 4

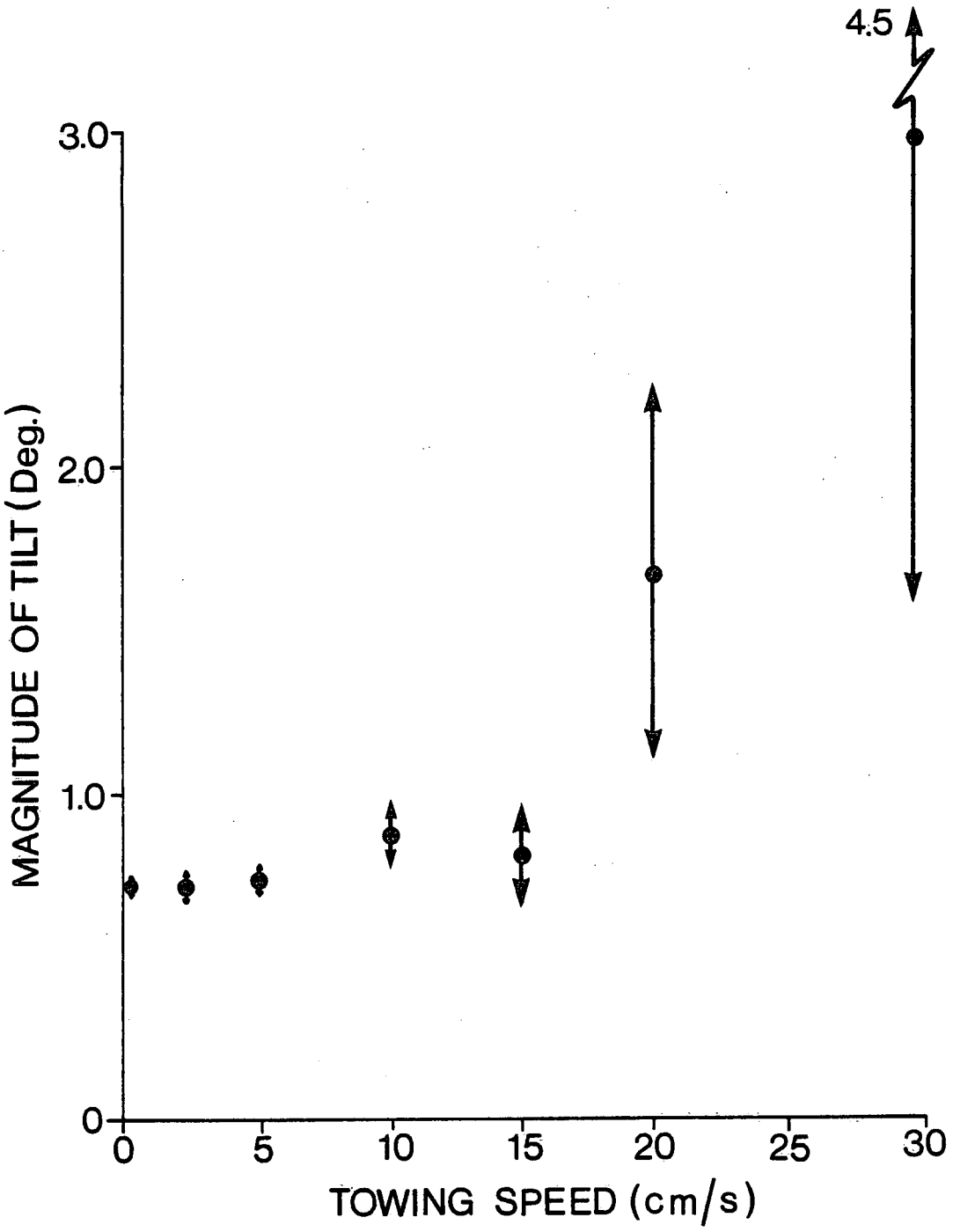
4.5
3.0
2.0
1.0
0
MAGNITUDE OF TILT (Deg.)
0
5
10
15
20
25
30
TOWING SPEED (cm/s)

FIGURE 5.

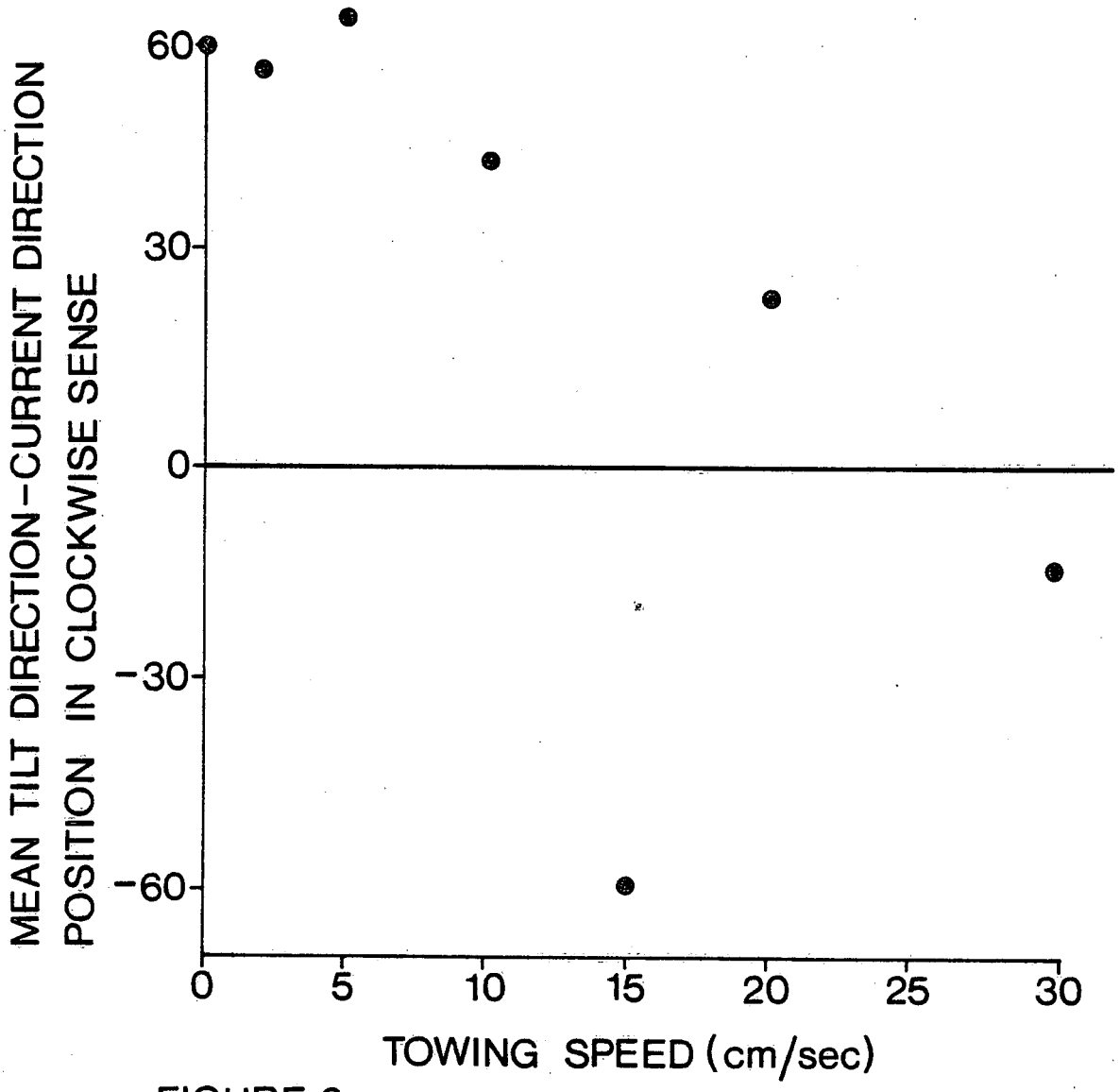
MEAN TILT DIRECTION-CURRENT DIRECTION
POSITION IN CLOCKWISE SENSE
60
30
0
-30
-60
0
5
10
15
20
25
30
TOWING SPEED (cm/sec)

FIGURE 6

TABLE 1

Towing Speed (cm/s)	Number Obs.	Depth		Compass (relative ^{o} N case)		Current Speed (cm/s)		Absolute Current Direction (^{o} N)		Tilt Angle (Degrees)		Tilt Direction (Degrees N)	
		Mean (m)	St. Dev. (cm)	Mean	St. Dev.	Mean	St. Dev.	Mean	St. Dev.	Mean	St. Dev.	Mean	St. Dev.
0	91	1.314	4.9	192	0.22	0.7	0.08	294	3.9	0.74	.01	353	0.7
2	312	1.383	6.8	189	2.3	2.73	0.24	289	3.4	0.73	.02	347	-
5	292	1.423	4.7	190	3.5	5.57	0.48	288	3.9	0.73	.02	350	3/5
10	293	1.423	5.1	191	7.8	9.4	1.06	289	8.0	0.87	.03	333	8.0
15	286	1.43	5.4	191	7.0	14.5	0.96	99	7.3	0.8	.04	389	7.4
20	181	1.444	6.4	186	7.7	21.6	2.7	286	8.5	1.7	.14	308	10.2
30	140	1.402	6.1	183	14.8	31.27	1.9	95	14.8	3.0	.36	80	17.8

rigging of the VAPS body is shown in figure 7 and is specifically designed to closely reproduce actual conditions of field deployment when the body is drawn very close to the bottom.

At the rest position, the body was displaced laterally with a pike pole and allowed to freely oscillate. Two modes of oscillation were observed. The first was a purely pendulum motion of about 3 complete cycles with a period of 6.5 seconds. Shortening the tether length to zero reduced the pendulum period to about 5 seconds. The second mode of oscillation was a very small rocking motion about the attachment of the tether to the bottom of the body. This damped out after only one or two cycles and was, in any case, of very small amplitude.

At steady towing speeds of up to 10 cm/sec, the body was much more stable than had been observed in the first towing tests. A pitching motion, with a period of about 6.5 seconds, which damped out after about 10 cycles, was observed upon starting the carriage from rest. At steady towing speeds of 10 to 20 cm/sec, the body began to rotate about its vertical axis. These torsional oscillations had a period of about 30 seconds and an amplitude of up to 100 degrees on either side of the mean current direction. At constant towing speeds of over 20 cm/sec, the body became very unstable with a combination of yawing, pitching, and rotating oscillations. The severity of these increased remarkably with increased speeds and frequencies, in some of the motions, as high as 1 or 2 Hz were observed.

In order to simulate wave motions, the body was quickly accelerated from rest to 50 cm/sec and then stopped. A number of these cycles were attempted, but the body itself was wildly unstable, and the test was discontinued for fear of damaging the body on the supporting structure.

The conclusion from the second tow tank drag test is that the body is adequate for measuring steady currents up to 20 cm/sec and is inadequate for measuring steady currents over 20 cm/sec or for unsteady (e.g. wave zone) flows at any speeds.

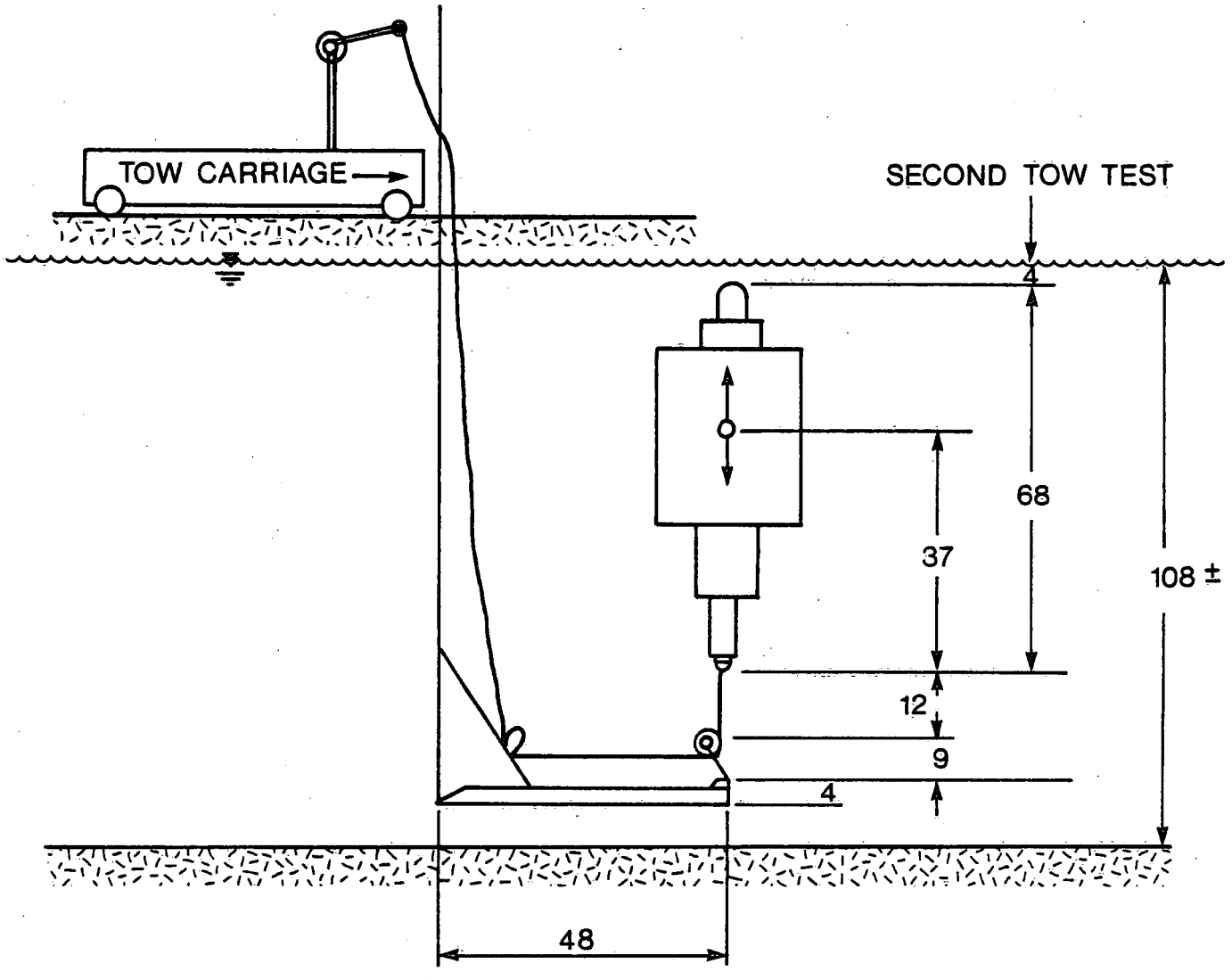

FIGURE 7

2. Lake Ontario Field Tests

The VAPS was installed in Lake Ontario approximately 40 metres from the existing tower in 12 metres of water. At the same time a current meter array of three Plessey current meters (sampling at 10-minute intervals) was installed on the tower to supplement an existing Marsh-McBirney E.M. current meter and a number of wave gauges. The experimental setup is shown in Figure 8. The proposed duration of the experiment was to have been 7 days.

2.1 Dwell Tests

At the depths of each of the three Plessey current meters, the VAPS body was dwelled for a period of 20 minutes, sampling at the rate of 0.5 Hz. The depths of the Plessey current meters were 1.5, 5.5, and 9.5 metres below the water surface, while the E.M. current meter was 6 metres below the surface. The VAPS body was profiled at various speeds throughout the same day (8 October, 1976). The data acquired from these experiments was logged on the First Field Tape. Following this experiment the VAPS body was profiled in its normal operating mode, and these data were logged on the Second Field Tape. A total of 150 profiles over a 14-hour period were collected. The failure of the control system after 14 hours is discussed separately.

Observations During Dwell Tests

During the Dwell tests, the wind was blowing from the north at approximately 4 m/sec. The r.m.s. wave height was about 0.58 metres, and the wave period was about 3.9 seconds. This gives a maximum orbital velocity, using linear wave theory, at the dwell depths of 17.0 cm/sec, 5.9 cm/sec, and 2.0 cm/sec at 2.5, 6.5, and 10.5 metres respectively. A typical wave spectrum at the tower, obtained at 0300, 9 October 1976, is shown in Figure 9.

In Figure 10, plots of the north and easterly current components measured by the VAPS are given for each of the Dwell tests. These plots are remarkable in that the currents at the bottom are much larger than those indicated for the top or middle dwell positions. Current Scatter diagrams are given in Figures 11, 12, and 13. The bottom scatter diagram shows evidence of a mean current directed along an onshore-offshore axis,

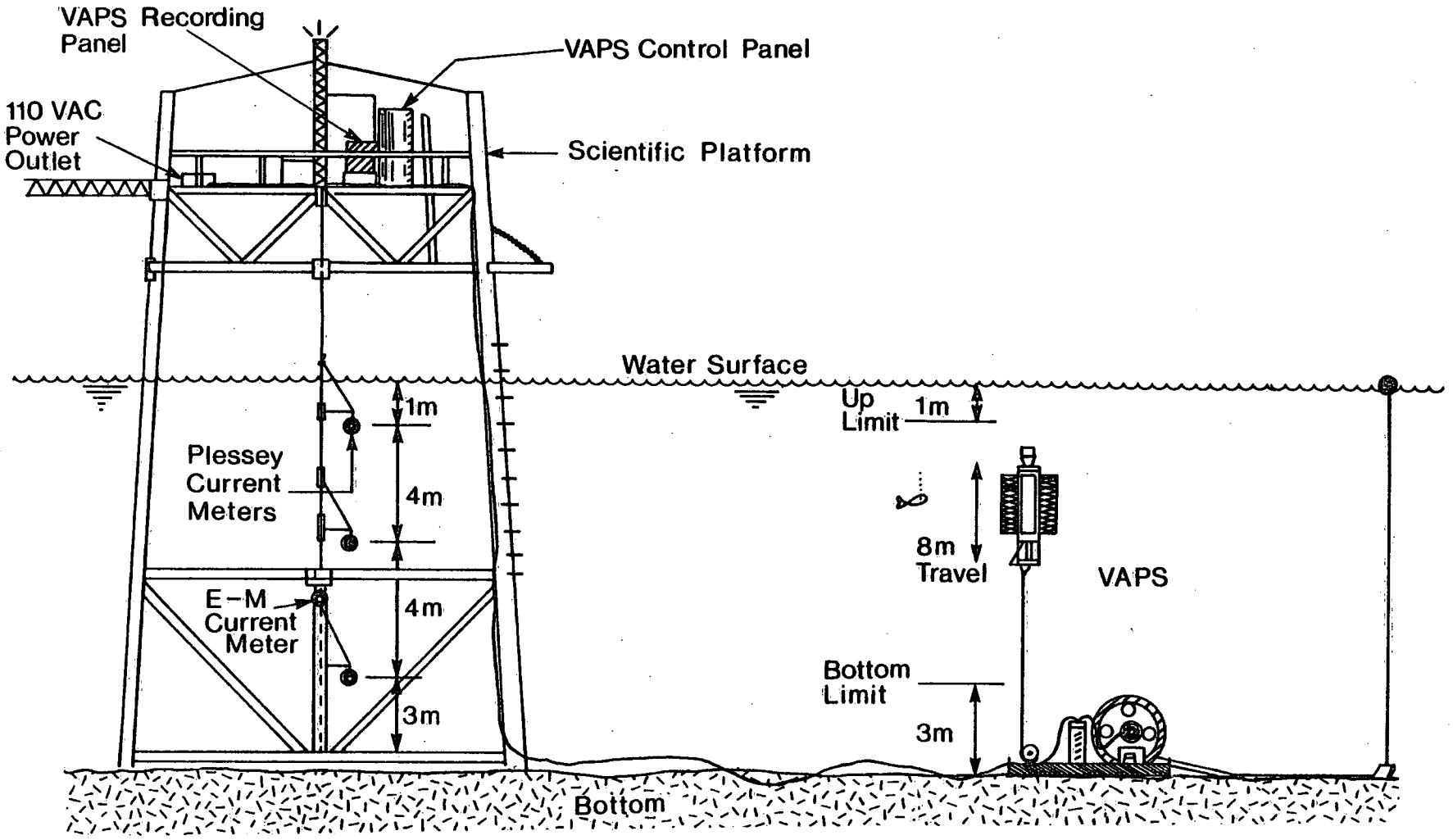

Figure 8. Lake Ontario Field Tests

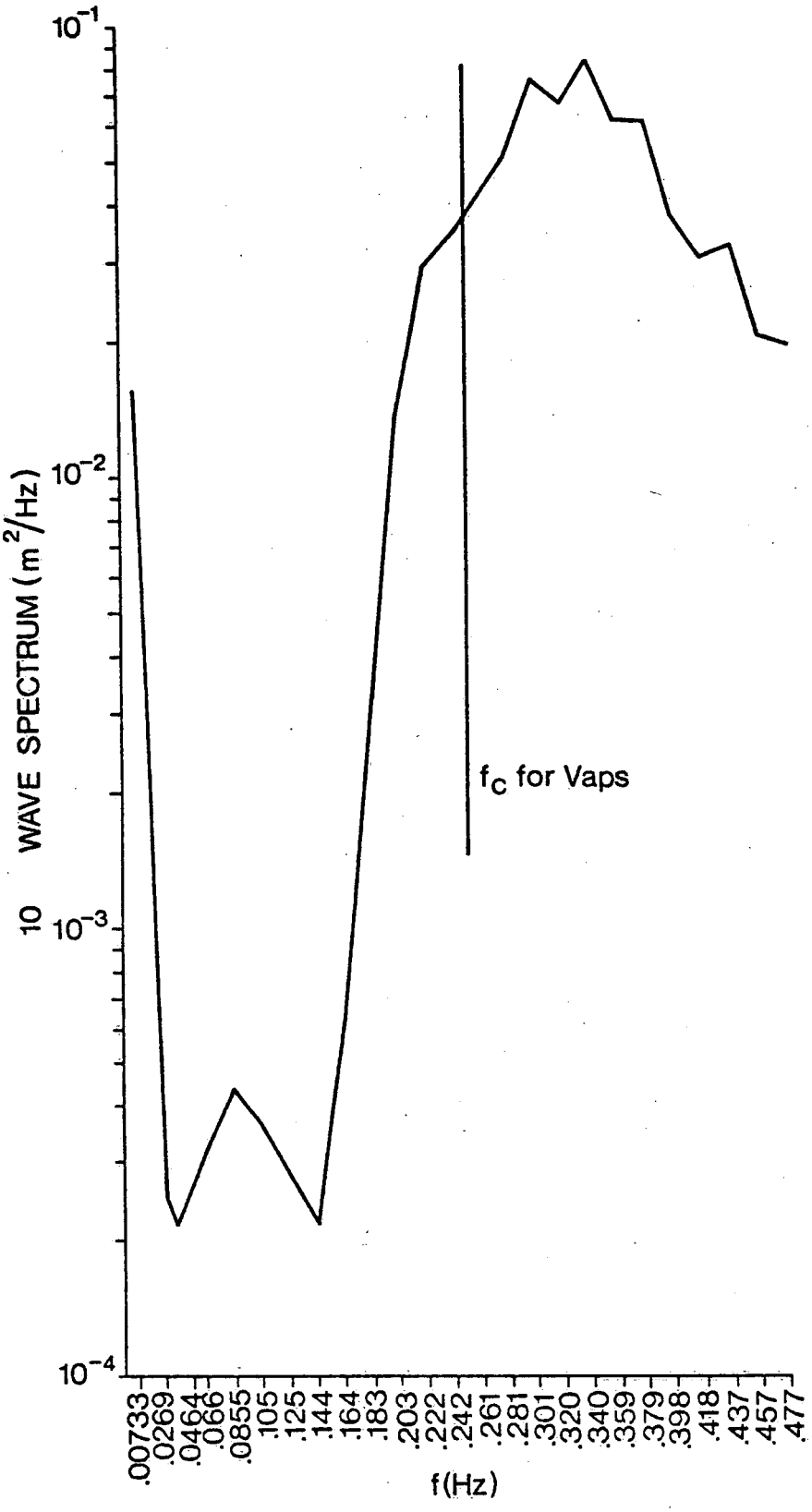

FIGURE 9. WAVE SPECTRA FROM TOWER 0300 AM 9 OCT/76

but the top and middle scatter diagrams would indicate a virtually random motion. The associated tilt scatter diagrams do not confirm this interpretation and are presented in Figures 14, 15, and 16. In the case of the tilt scatter diagrams, it seems evident that the tilts, although having a somewhat random component, are directed primarily along an onshore-offshore axis. From the evidence of the wave data and the tilt data, it would seem reasonable to believe that there is an onshore-offshore current pattern and the acoustic current sensor is not recording this current at the top and middle dwell positions. It is evident that there is a progressive degradation in the acoustic current meter results as the body approaches the surface.

Since certain periodicities can be seen in the component plots of the acoustic current meter speeds, the dwell records were subjected to spectral analysis. Some of the results of these analyses are shown in Figures 17, 18, 19, and 20. In all cases, the plotted spectra have been normalized such that the total variance is 100. The total variance for each parameter at each depth is provided in the figure for reference.

In all of the spectra, a large energy peak can be observed at 5 seconds. At first it was thought that this was the wave energy folded back beyond the Nyquist frequency of 0.25 Hz; however, for both the tilt amplitude and the current amplitude, this 0.20 Hz energy increases with depth while the wave energy clearly decreases exponentially with depth. A more plausible explanation is that the resonant frequencies observed in the tow tank are being excited at the bottom dwell position while most of the folded wave energy in the top position is not being recorded by the speed sensor, since the body is moving with the waves, and so there is very little energy at the top position relative to the body.

It was observed in the second tow tank test that, in a varying flow field, the body essentially moved with the flow field so that there was only a small current relative to the body, while at the same time the body exhibited large torsional oscillations. The spectra of the current speeds bear this out, since they show much less energy at the top dwell position than at the bottom dwell position.

The means and the standard deviation of the current speed and direction and the tilt amplitude and direction were calculated in geographic

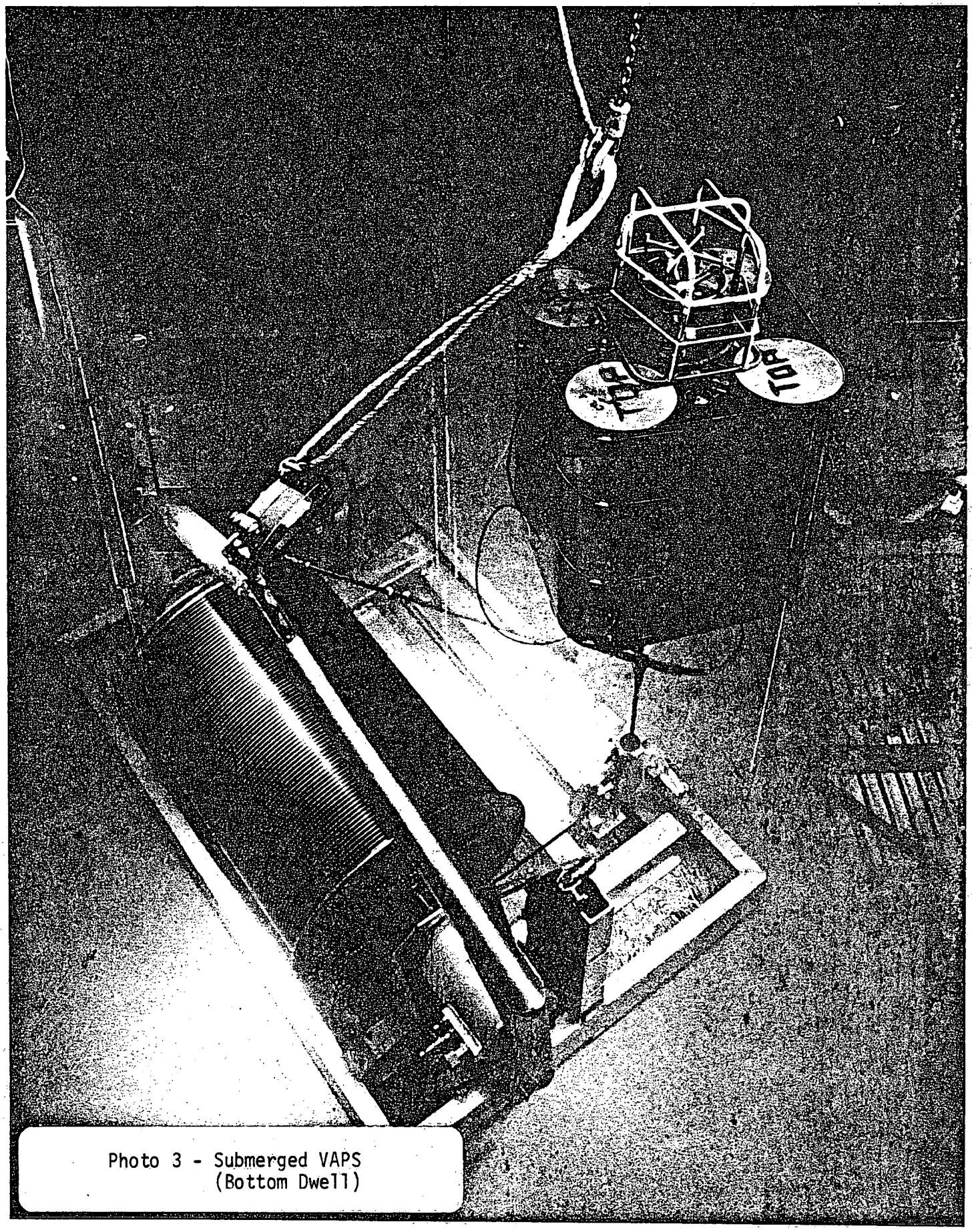

Photo 3 - Submerged VAPS
(Bottom Dwell)

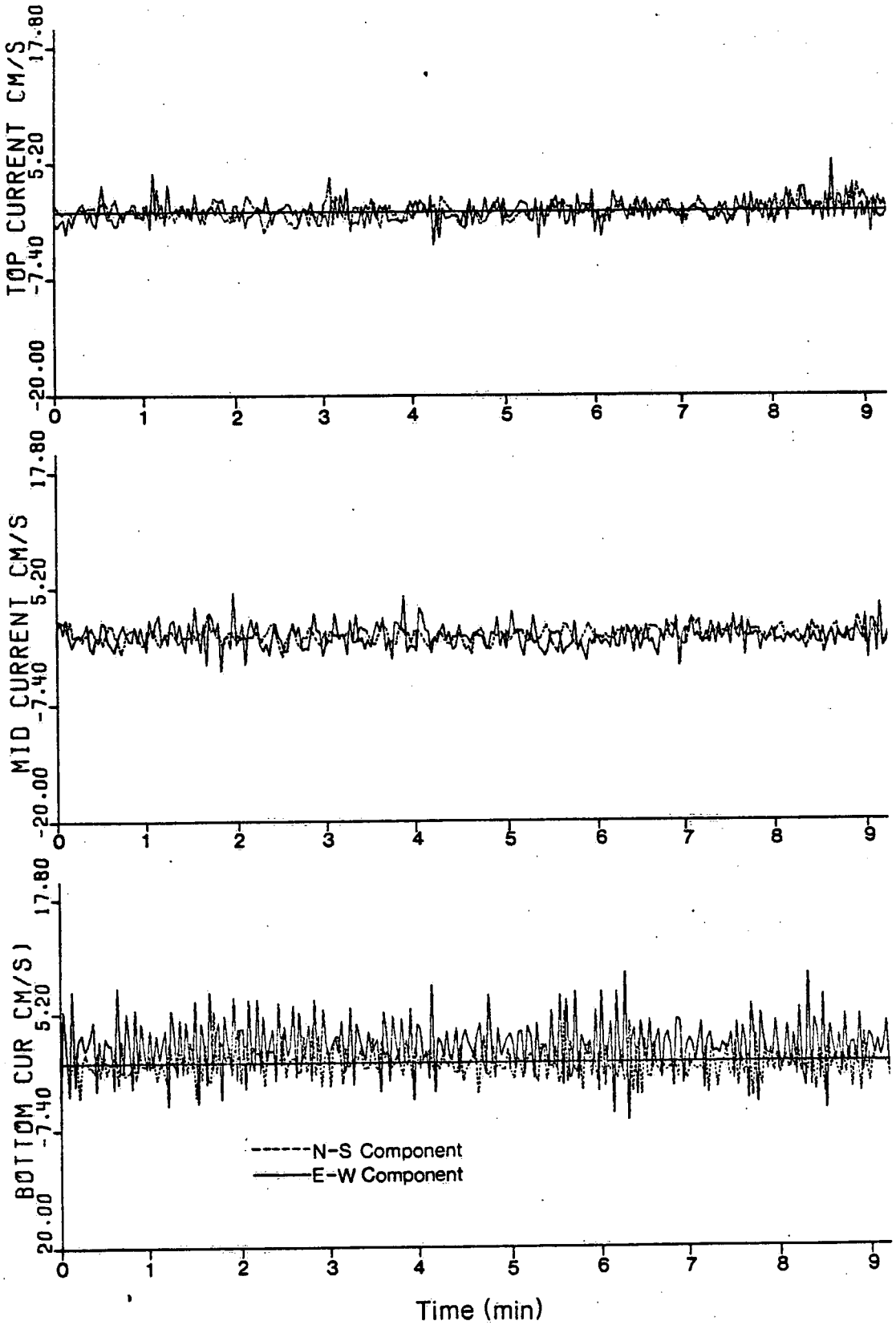

Figure10 VAPS CURRENT SPEED MEASUREMENTS (DWELL TESTS)

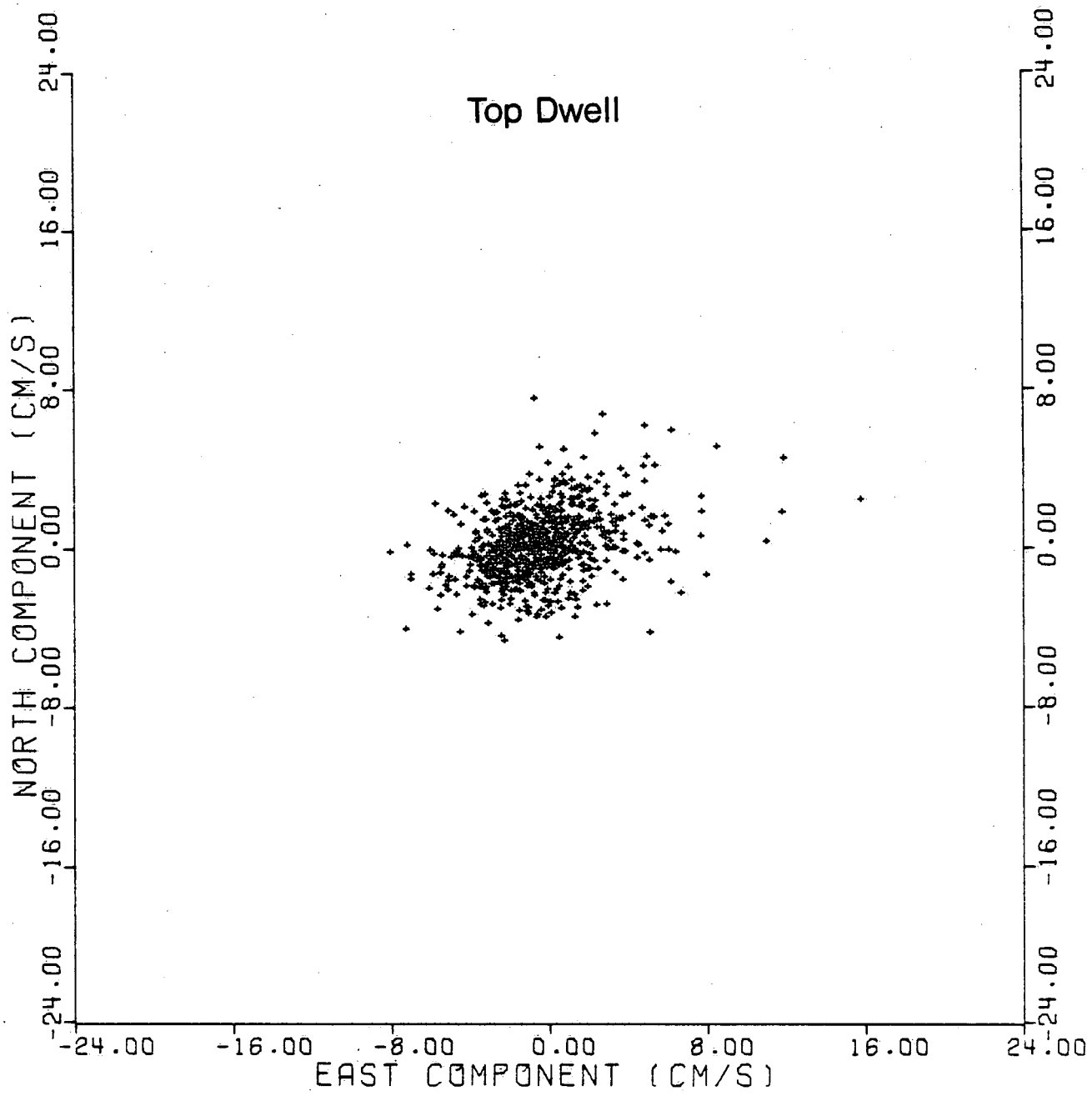

Figure 11 VAPS ACOUSTIC CURRENT METER SCATTER DIAGRAMS

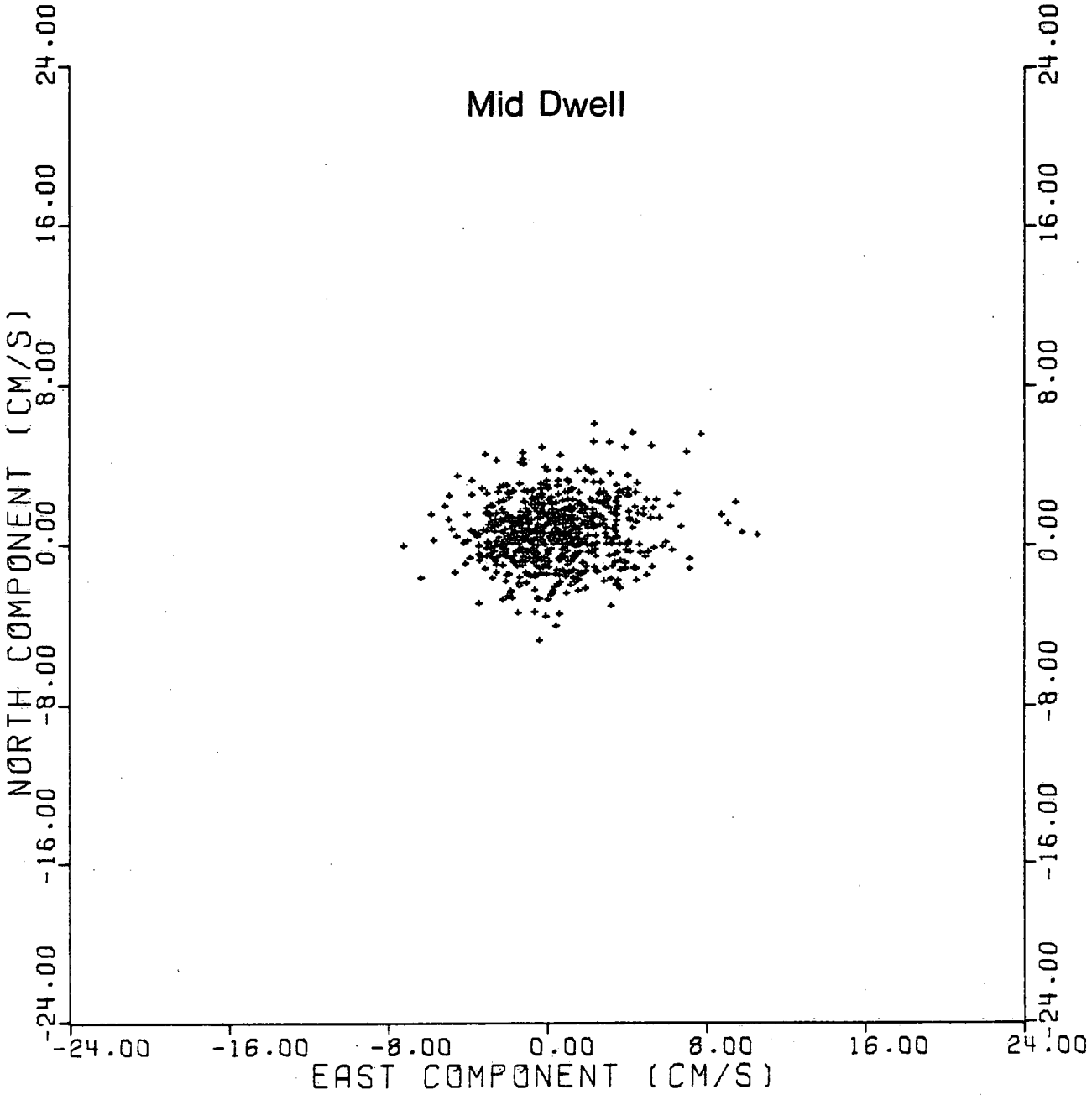

Figure 12 VAPS ACOUSTIC CURRENT METER SCATTER DIAGRAM

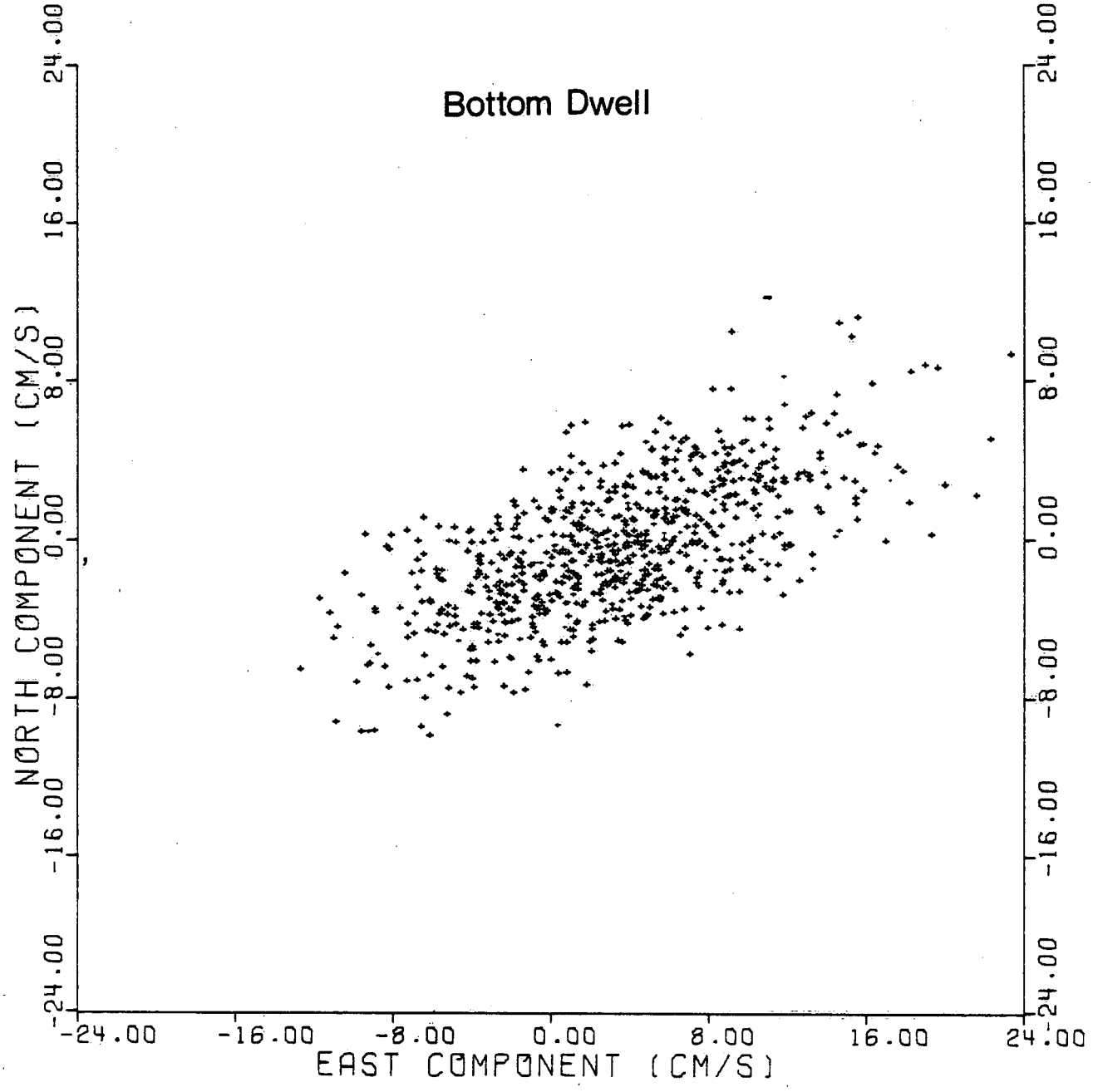

Figure 13 VAPS ACOUSTIC CURRENT METER SCATTER DIAGRAM

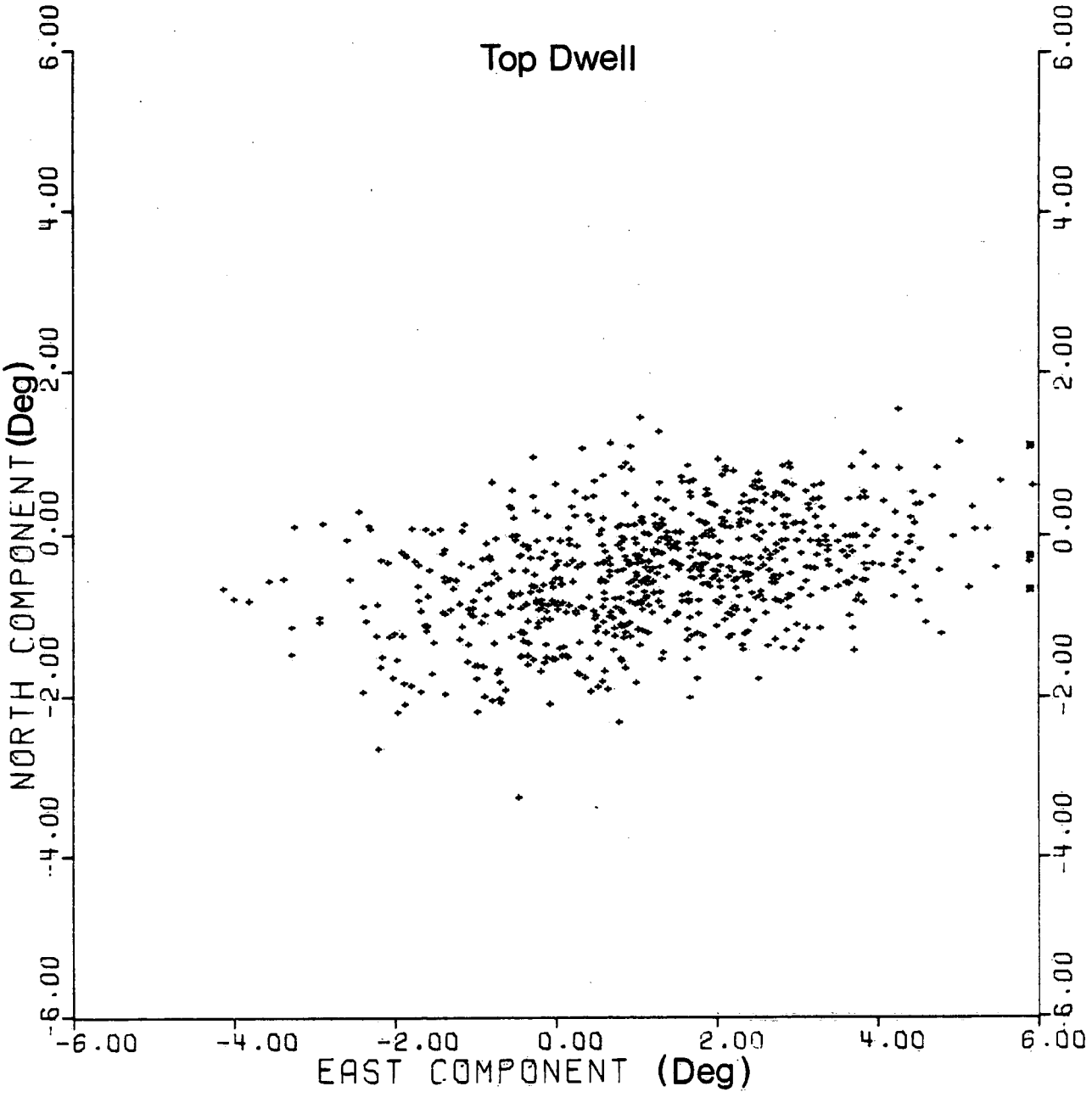

Figure14 VAPS TILT SENSOR SCATTER DIAGRAM

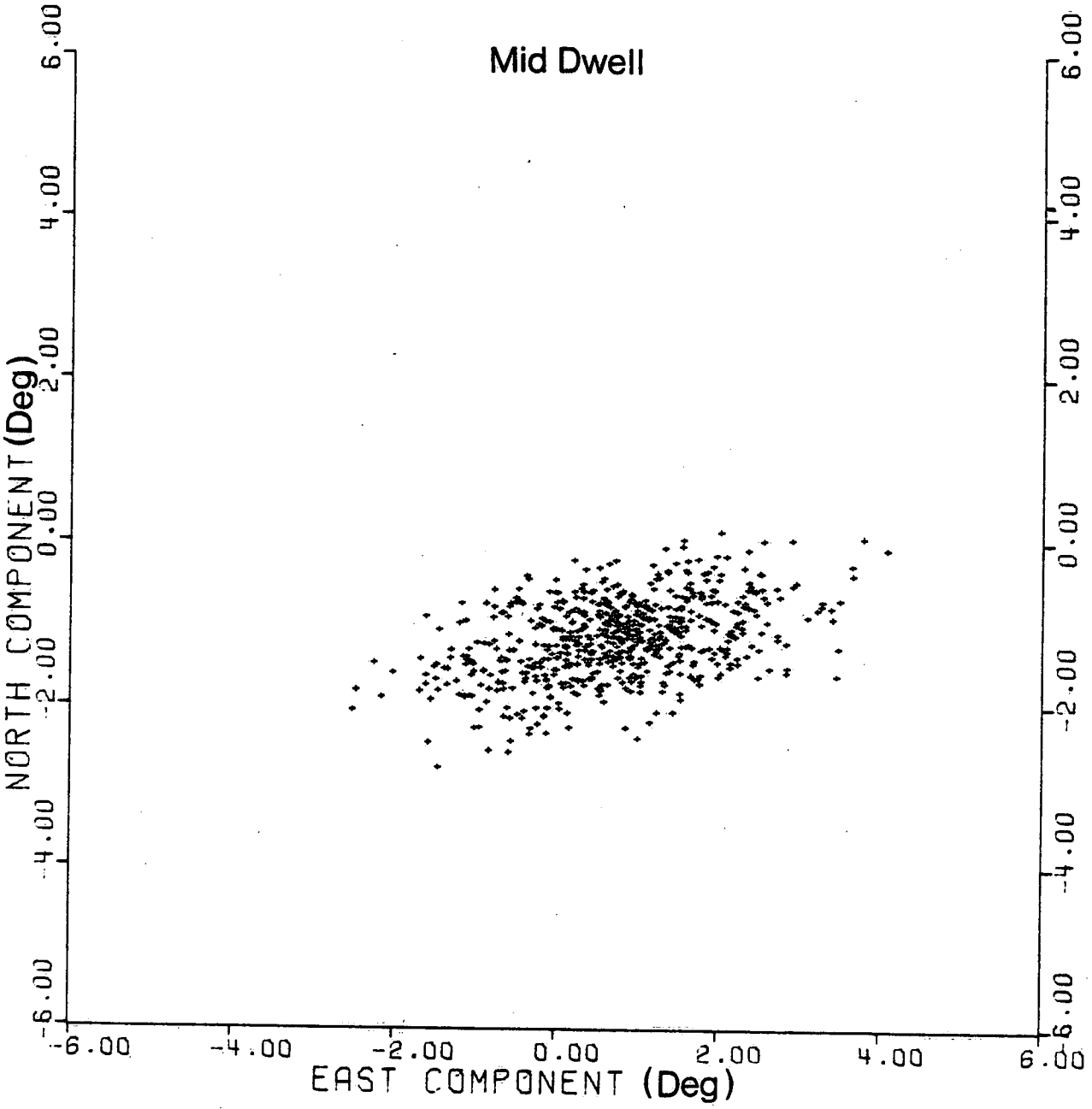

Figure 15. VAPS TILT SENSOR SCATTER DIAGRAM

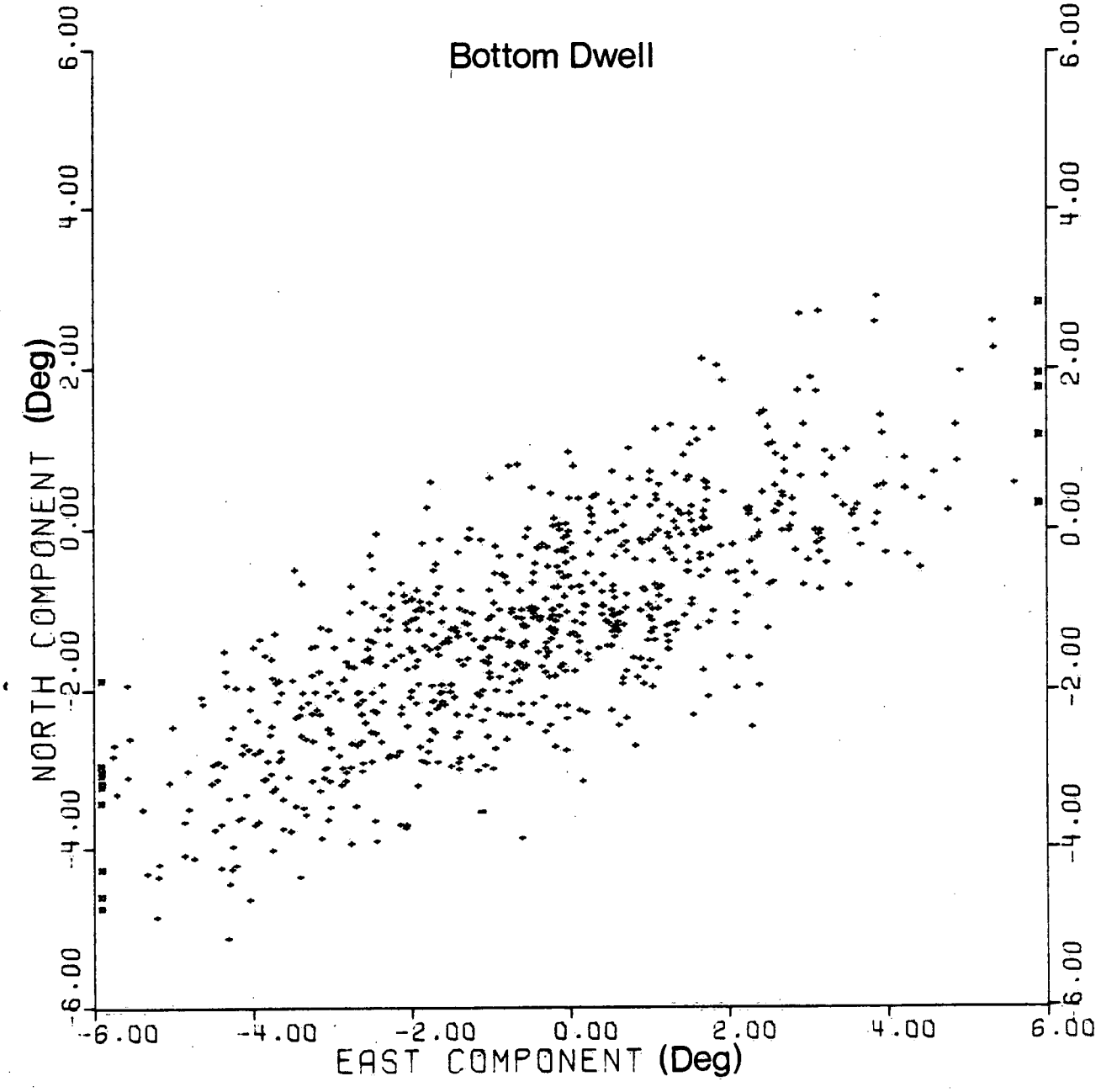

Figure 16 VAPS TILT SENSOR SCATTER DIAGRAM

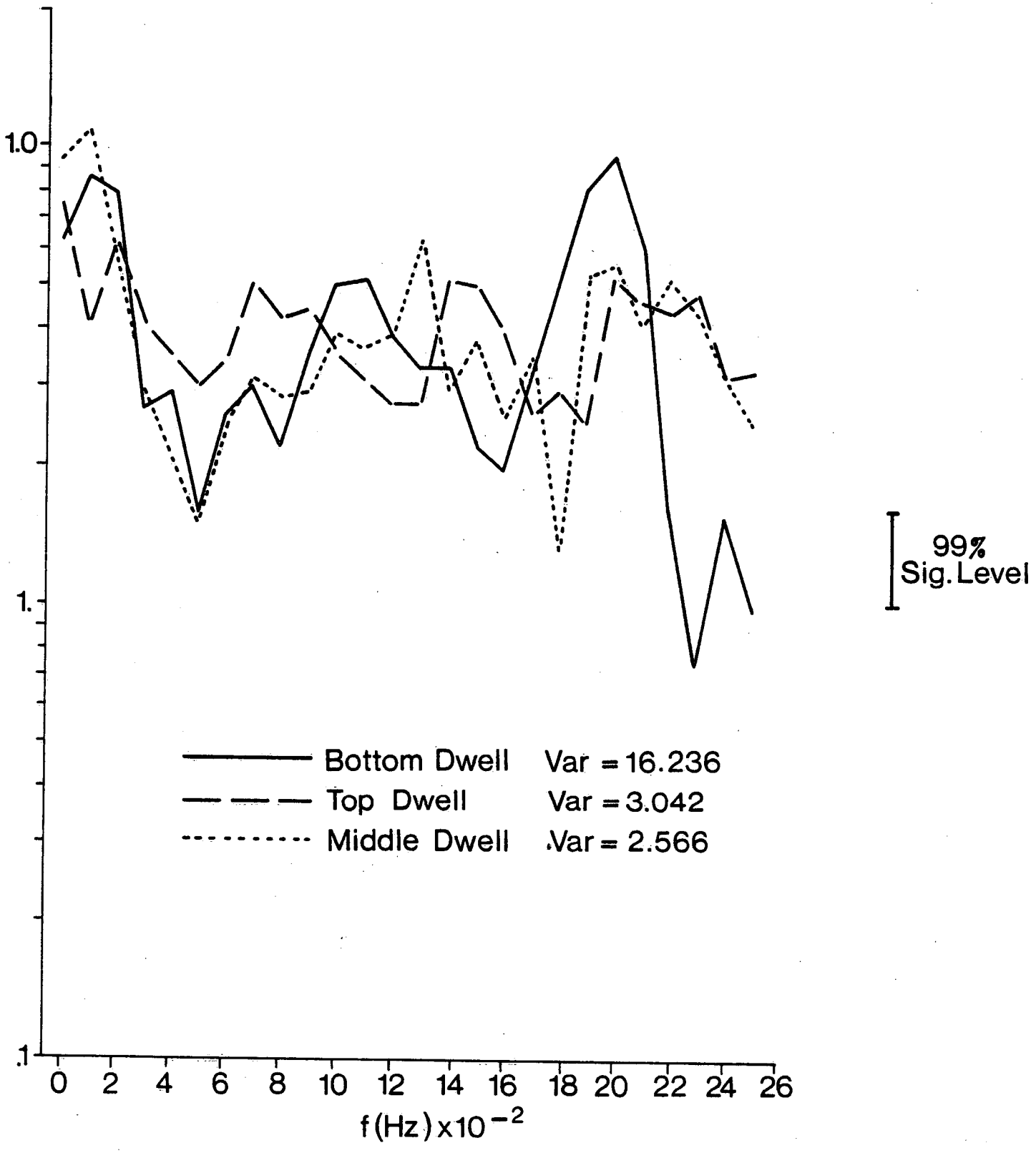

FIGURE 17. VAPS DWELL TESTS NORMALIZED AUTO SPECTRA CURRENT AMPLITUDE (Body Co-Ordinates)

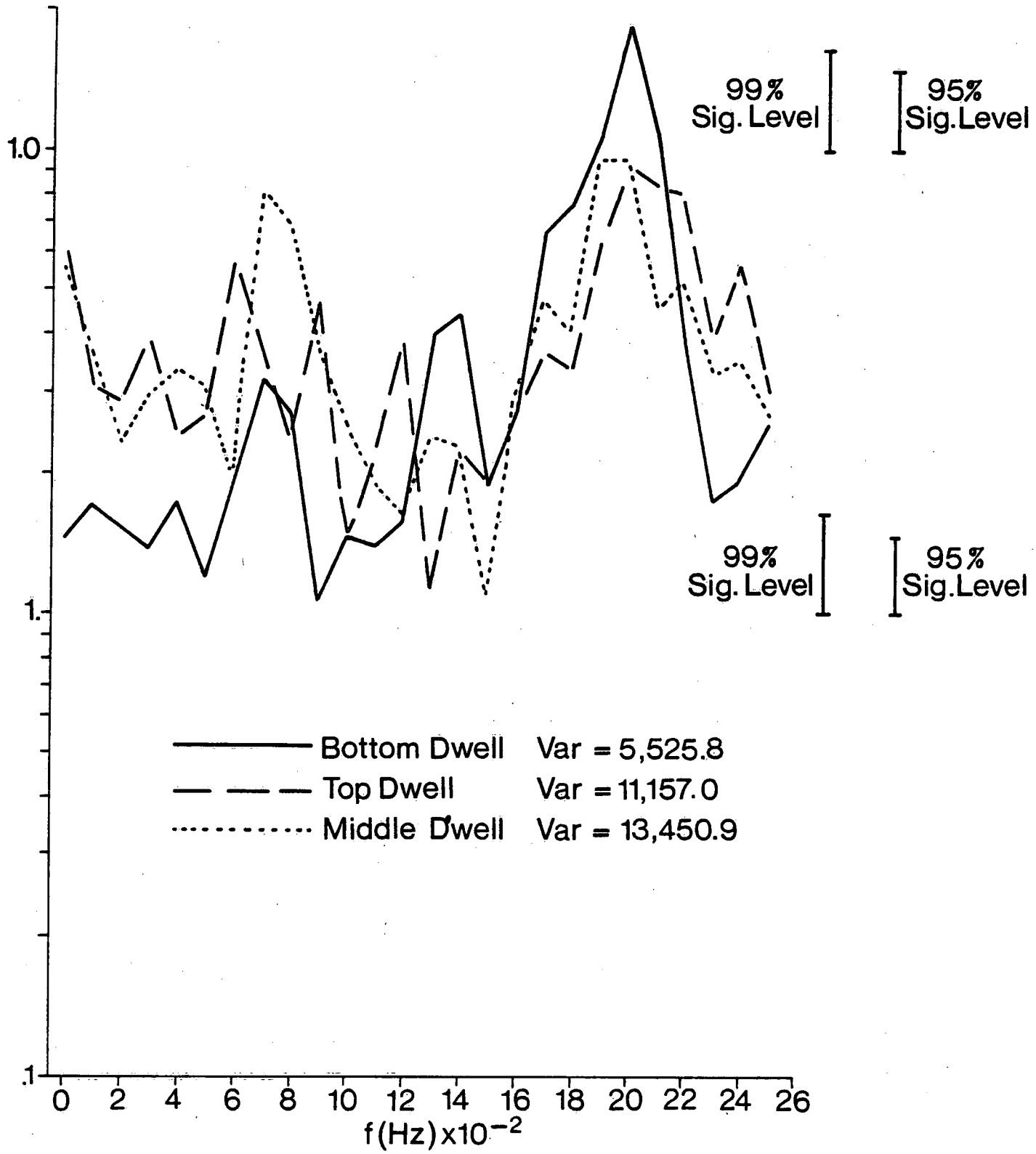

FIGURE 18. VAPS DWELL TESTS NORMALIZED AUTO SPECTRA OF CURRENT DIRECTIONS (Geographic Co-Ordinates)

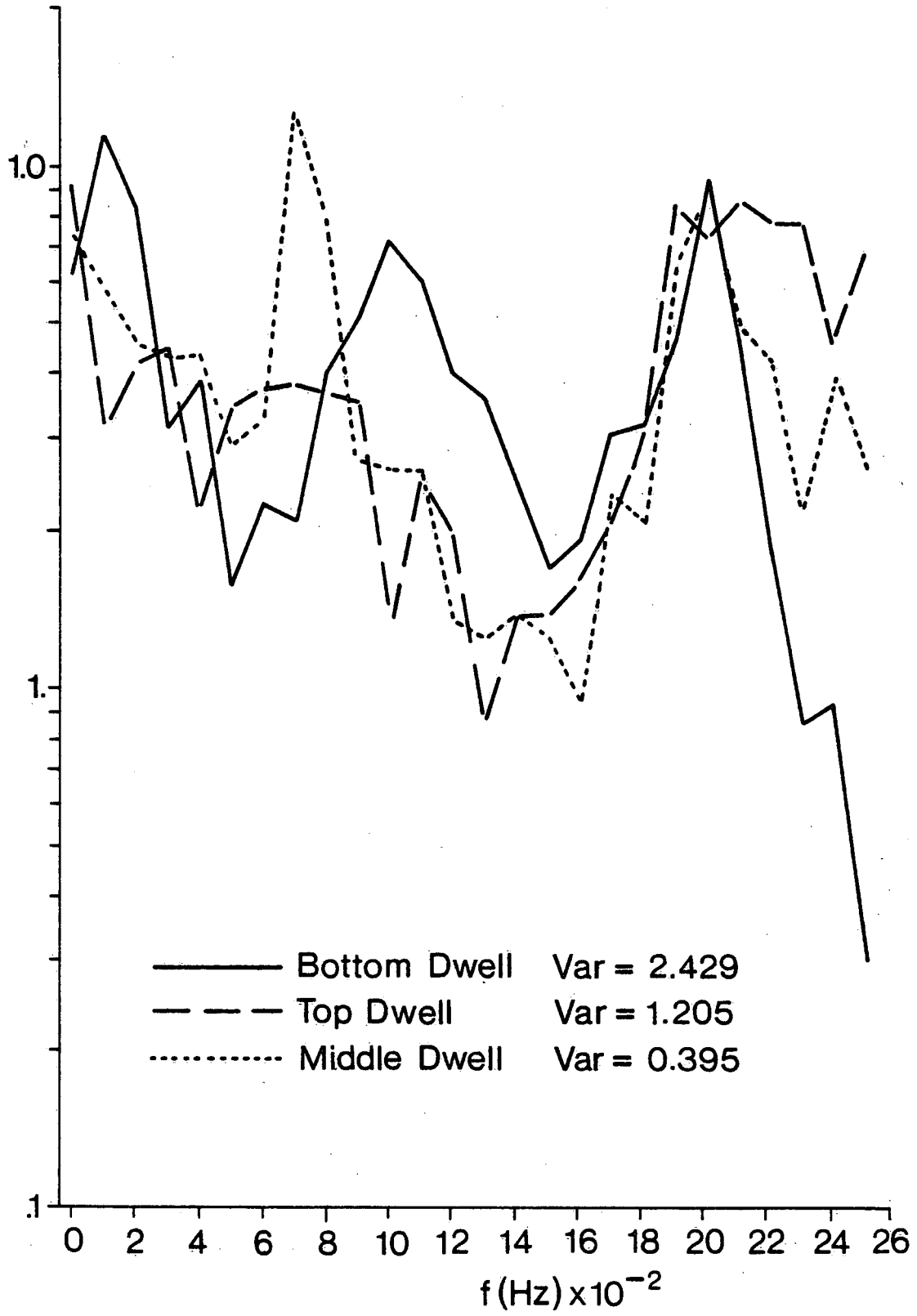

FIGURE 19. VAPS DWELL TESTS NORMALIZED AUTO SPECTRA TILT AMPLITUDES

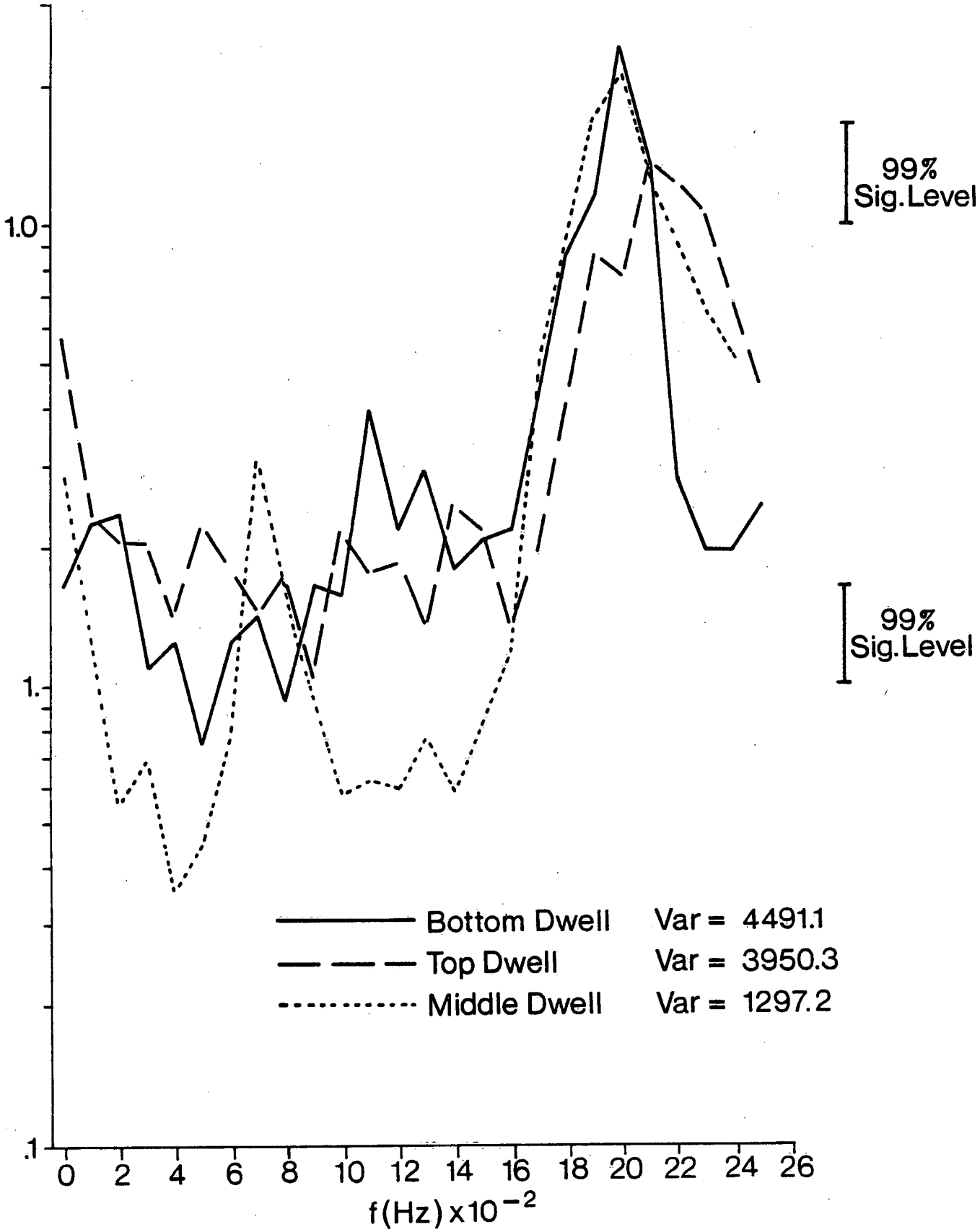

FIGURE 20. VAPS DWELL TESTS NORMALIZED AUTO SPECTRA OF TILT DIRECTIONS (Corrected For Compass)

DWELL TEST STATISTICAL DATA

Parameter		Nominal Depth (m)		
		2.5	6.5	10.5
Max. Orbital Velocity (cm/sec)		17.0	5.9	2.0
E.M.C.M. @ 5 m:	Spd		2.9	
(Mean Velocity)	Dir		168°T	
Plessey C.M.	Spd	8.0	3.9	3.3
(Mean Velocity)	Dir	204	180	187
VAPS Measured Depth	Mean (m)	2.42	6.59	10.62
	St. Dev. (m)	0.103	0.055	0.06
VAPS Measured Temperature	Mean (°C)	11.65	11.62	11.40
	St. Dev.	0.004	0.008	0.090
Plessey Measured Temperature	Mean (°C)	11.7	11.8	11.0
Acoustic Mean Speeds (cm/sec)	East/Spd	-0.48 / 0.52	0.38 / 0.81	3.34 / 3.36
Geographic Coordinates	North/Dir	0.21 /293.6	0.71 / 28.2	-0.40 / 96.8
Acoustic Mean Speeds (cm/sec)	East/Spd	0.534/ 0.64	0.135/ 0.81	0.190/ 3.35
Body Coordinates	North/Dir	0.352/ 46.61	0.801/ 9.61	3.346/ 3.3
STD Dev. Speeds	East	2.61 / 2.52	2.48 / 2.05	6.13 / 4.12
Geographic/Body	North	1.71 / 1.80	1.58 / 2.11	3.42 / 5.69
Mean Tilt (Degrees)	East/Amp	-0.536/ 1.37	-0.486/ 1.37	-0.466/ 1.38
Body Coordinates	North/Dir	1.262/337.0	1.286/339.3	1.297/340.2
Mean Tilt	East/Amp	1.24 / 1.32	0.74 / 1.40	-0.61 / 1.4
Geographic Coordinates	North/Dir	-0.45 /110	-1.19 /148	-1.26 /206

TABLE II: Speeds in cm/sec, Tilts in Degrees, Directions in Degrees True. All means are vector means.

coordinates and in body coordinates. The difference is that the compass readings are used to reduce the body coordinates to geographic coordinates. This allows an examination of the compass and the body performance. By examining the standard deviations in body coordinates of the acoustic mean speeds in Table II, it is evident that either the flow field is either very random or else the body is rotating quite badly. The second tow tank test has shown that the body does rotate quite badly in unsteady flow fields, and so a good check on the compass performance is to compare the Plessey directions with the acoustic current directions. The large discrepancies here indicate that the compass does not perform well, and later tests show that the time response of the compass is about 4 seconds. It is then not surprising that there is very little agreement between the Plessey directions and the VAPS directions in any of the Lake Ontario Tests.

It is difficult to assess the temperature sensor except to say that it yields more reasonable results than does the Plessey sensors. It is evident that the water column is very well mixed, but the Plessey sensors indicate a temperature reversal with depth, which is difficult to believe.

The results from the tilt sensor were not too useful. In terms of body coordinates, there seems to be a very small mean tilt of exactly 1.37 degrees at all depths. The magnitudes of the tilts were always very small, and they did not seem to correlate well with any easily observable phenomenona.

2.2 Profile Tests

1) Profiling Tests

The profiler was successfully operated in its standard profiling mode for about 150 complete profiles over 14 hours.

2) Profiling Rate Tests

Profiles were taken at several different vertical speeds of 2, 5, 10, and 15 cm/sec, while recording on cassette and monitoring the full sensor suite.

On the last day of field tests, after a holiday weekend of unattended operation, the vehicle was discovered floating on the surface and about 40 metres of cable had paid out.

a) Diving inspection revealed that the slack tether cable had entangled around the winch components on the bottom.

b) Upon retrieval, the system was quickly refurbished and proved to still be in working order.

c) Analysis of the data output from the cassette revealed that the system malfunctioned about 04:00 hrs. on Saturday, October 9, 1976. At approximately 5½ minutes per profile, the estimated 12 hrs. of good operation beginning Friday, October 8, provided 130 profiles.

d) The problems have been addressed by further cold temperature tests and pull tests on the winch and examination of noise problems with the SCR controller.

Observations and Results from First Field Tape

Individual current vectors are plotted in planar form in the diagrams of Figures 21 and 22. The origin of the current vector is situated at the appropriate position in depth and time. North is vertically up and east to the right.

Temperature and tilt profiles are plotted in the bottom panels of Figures 21 and 22.

In general, the profile results conform to those of the dwell experiments. At the surface, the currents are noticeably weaker than at the bottom (Figure 21). The currents are evidently highly variable in direction, so much so that no regular pattern is discernable. The temperature profiles are nearly isothermal. Tilts vary from nearly zero to several degrees as was the case in the dwell experiments.

A number of profiles were taken at ascent rates other than 5 cm/sec. Figure 22 demonstrates several selected current measurements at an ascent rate of 15 cm/sec. In general, no influence of profiling speed at this speed or at 10 cm/sec could be detected. There is a suggestion that the tilt may be stabilized somewhat at the higher profiling speed.

Depth variations in the profiling mode are comparable to those experienced in the dwell tests. Apparent reversals in depth are particularly evident at the surface position (Figure 21).

A complete current profile from the surface to the bottom is shown in Figure 23, and a complete profile of temperature and tilt is

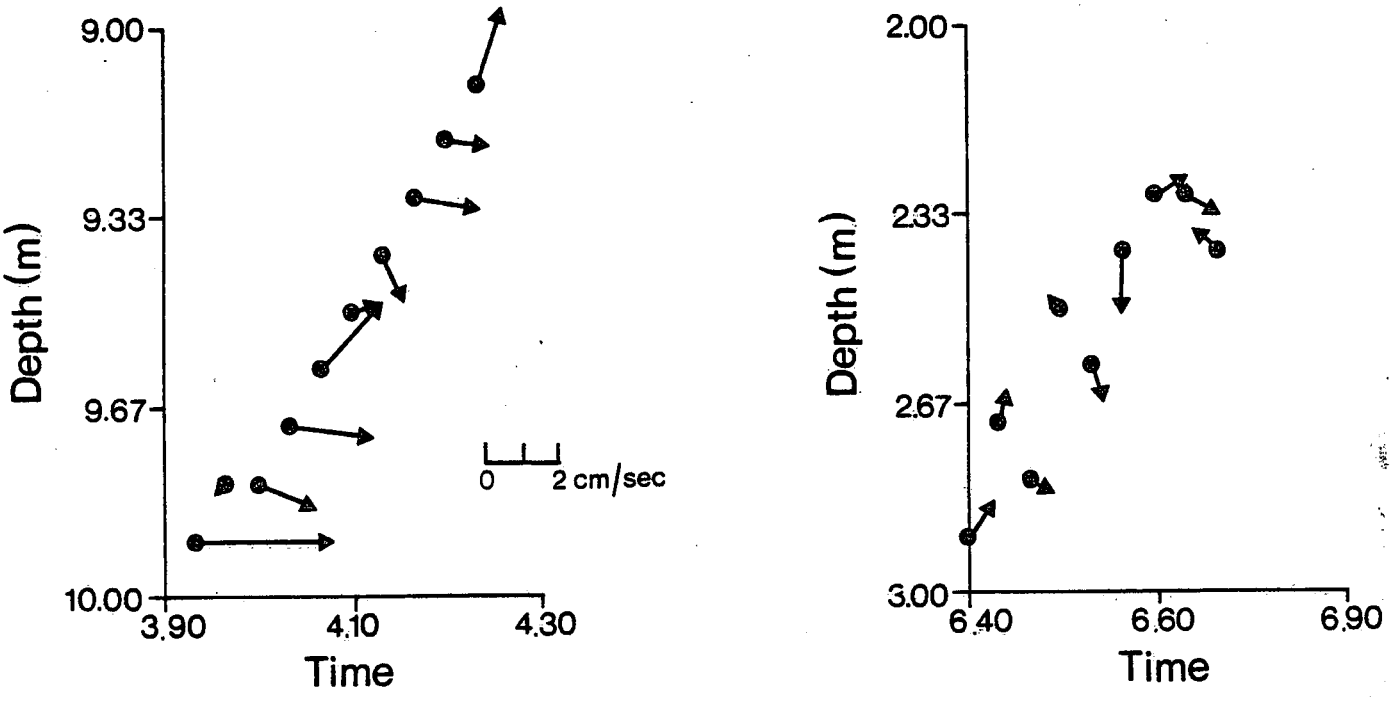

(a) Current Speeds

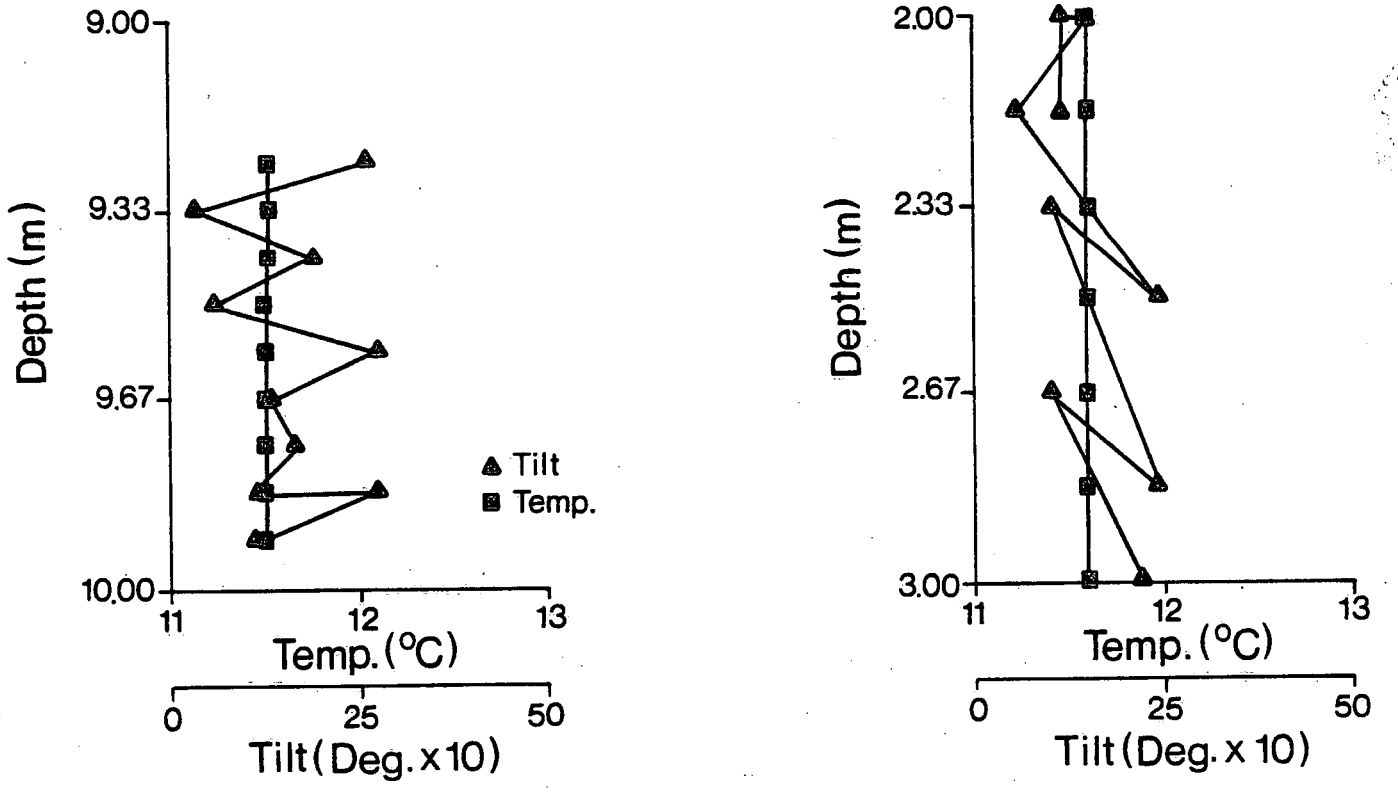

(b) Temperature and Tilt

Figure 21 PROFILING at 5 cm/sec

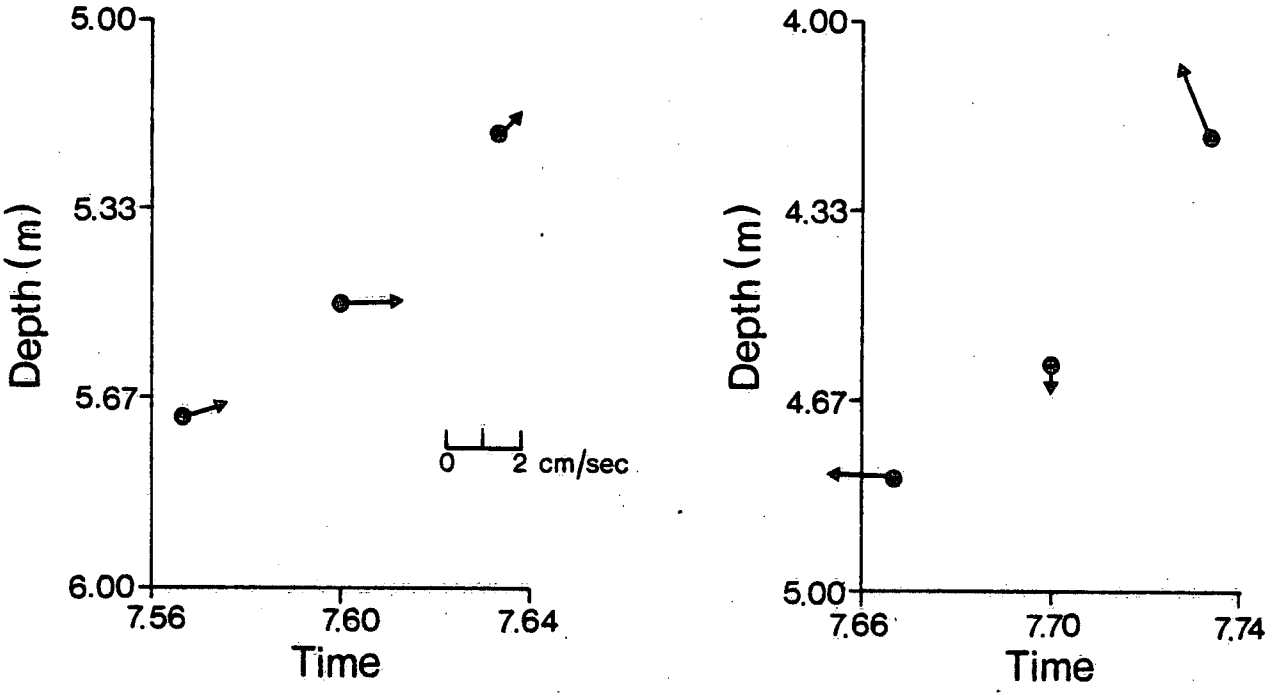

(a) Current Speeds

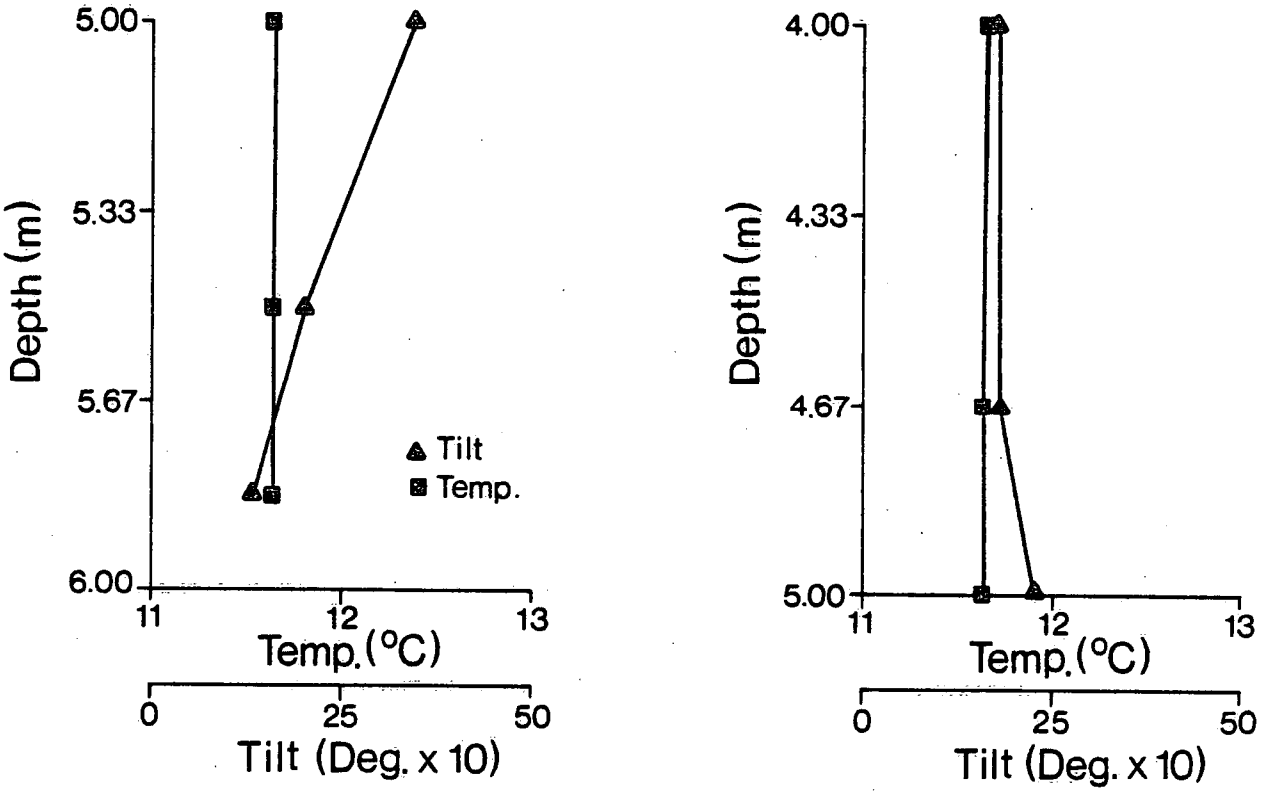

(b) Temperature and Tilt

Figure 22 PROFILING at 15 cm/sec

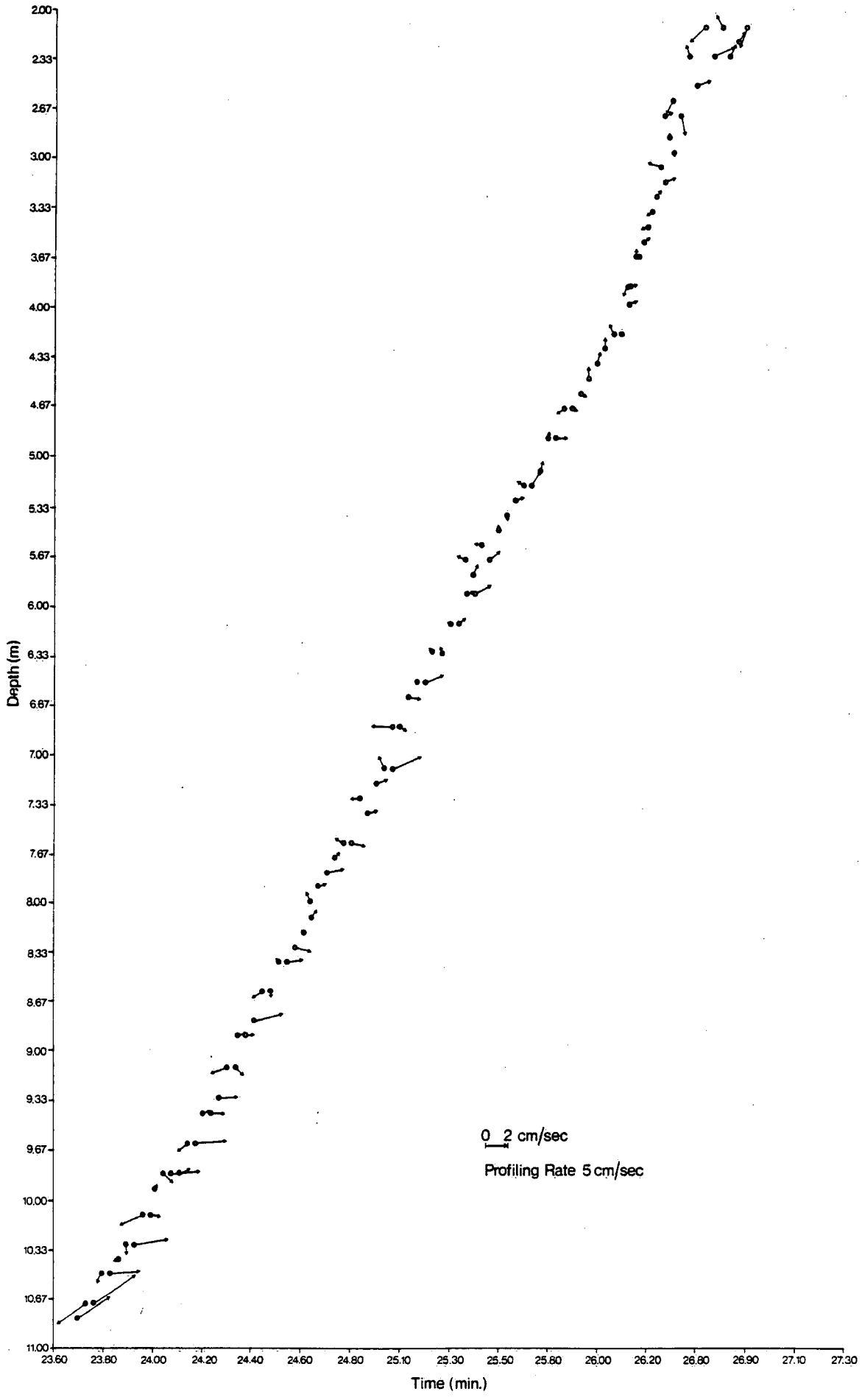

Figure 23 CURRENT SPEED vs DEPTH

shown in Figure 24.

Profiles were also plotted of the quantities vector averaged over one-metre intervals in the vertical. Considerably more regularity is observed in the current vectors from profile to profile in this case.

2.3 Second Field Tape

The second field tape contains 14 hours of continuous profile data collected at the tower site after the dwell tests and initial profiling tests were completed. These data were analyzed for two major reasons. The first is that a rather curious thermal event occurred over this 14-hour period, and the second reason is that accurate wave data are available for the period.

Figures 25, 26, and 27 show the establishment of the thermal structure and its disappearance. On these plots, the readings were vector-averaged over each metre of depth, and the Plessey current meter vectors are also plotted for the sake of comparison. Although at first sight the acoustic current meter vectors seem to have little in common with the Plessey current vectors, the temperature plots indicate the value of the VAPS concept; since, over the one metre averaging, the temperature structure is very well defined. At the end of the episode, where the currents seem to be fairly strong throughout the water column (Figure 27), it should be noticed that the acoustic current meter results do correspond fairly closely to the Plessey current vectors at the mid and bottom depths.

Figure 28 shows the fine temperature structure in the 10-11 metre depth interval during the cold-water intrusion episode. The VAPS indicates a curious inversion of over $1^{\circ}C$ at the bottom of the profile. This inversion is not isolated to one profile but extends over nearly all profiles during this cold temperature event. The Plessey temperature is $1.5^{\circ}C$ colder than the VAPS temperature sensor which indicates a fairly large discrepancy. It is thought that there is some lagging of the VAPS temperature sensor which causes this, but the problem has not been rectified as yet.

During the period in which the data for the second field tape were collected, accurate wave data were also collected. From linear wave theory we have that at any depth, z, the maximum orbital velocity of

the wave is:

$$u_{max} = u_o e^{-kz}$$

where: $u_o = h/2\sqrt{kg}$, $k = 2\pi/L$

and g = acceleration due to gravity;

h = r.m.s. wave height;

T = wave period; and

L = wave length.

Table III contains data collected during the period of the second field tape. The wave velocity is the calculated velocity present at the depth due simply to wave motion. The Plessey current meter speeds do not contain any of this wave velocity, while the acoustic current speeds contain not only the mean current but also a component of the orbital velocity. Although there is very little correspondence between the Plessey directions and the VAPS directions, the speeds fare much better.

Figure 29 gives a plot of the Plessey speeds versus the Acoustic current meter speeds for the 6.5 and the 10.5 metre depths. A perfect correspondence would be given as a line with a slope of 45°. If the wave orbital velocities are considered as error bars on the Plessey values, there is excellent agreement between the VAPS values and the Plessey values except for VAPS speeds less then 2 cm/sec, which is the threshold speed for the Plessey current meter. The lack of agreement in the directions is not surprising considering the motion of the body that was observed during the second Tow Tank Tests.

In Figures 30 to 32 contoured plots of the thermal and velocity structure as a function of time and depth provide a picture of the growth and disappearance of the cold water intrusion. At the onset and at the end of the episode, nearly isothermal conditions prevail. Gradual cooling is evident in the upper layer. Onshore velocities at the bottom are consistant with the bottom cooling at the beginning of the intrusion, while offshore velocities agree with the bottom warming at the end of the period. Stronger longshore currents are found in the bottom portions of the plot (Figure 31).

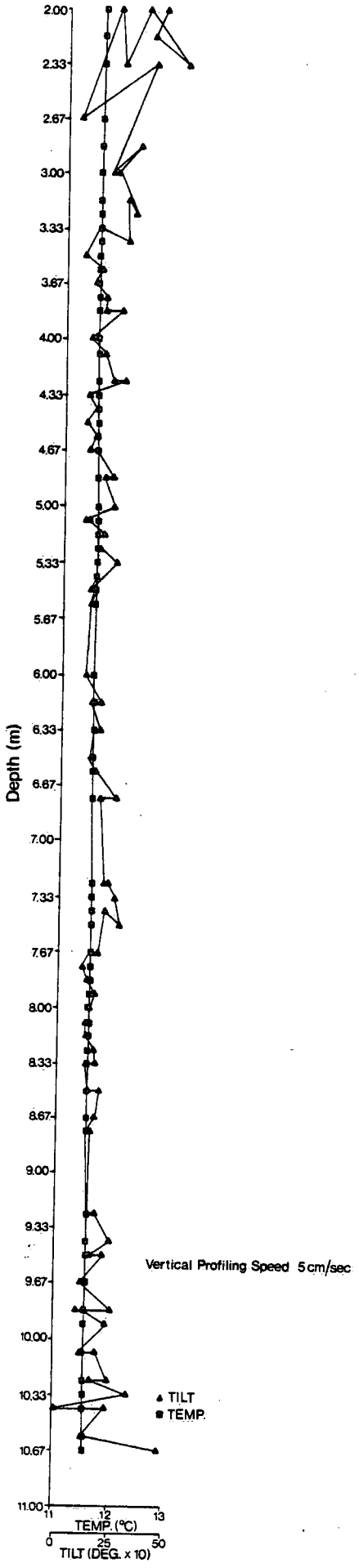

Figure 24 TEMPERATURE and TILT vs DEPTH

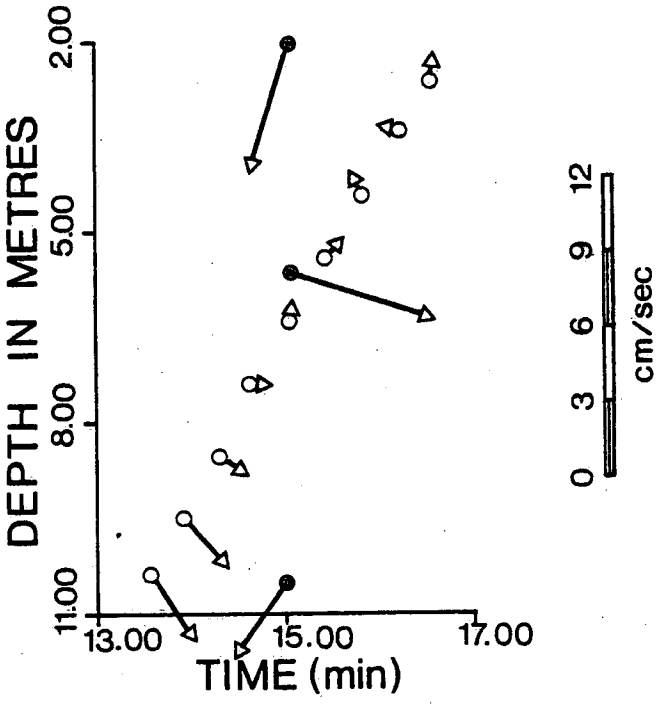
DEPTH IN METRES
2.00
5.00
8.00
11.00
13.00
15.00
17.00
TIME (min)
0
3
6
9
12
cm/sec

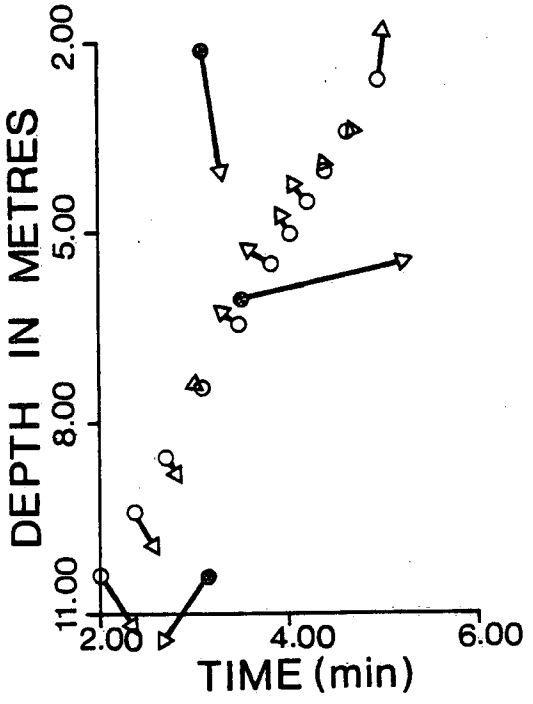
DEPTH IN METRES
2.00
5.00
8.00
11.00
2.00
4.00
6.00
TIME (min)

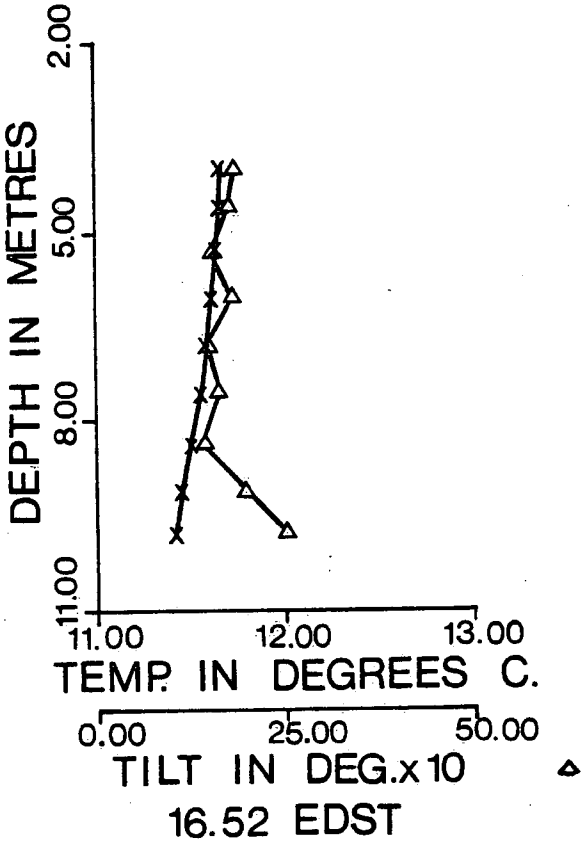
DEPTH IN METRES
2.00
5.00
8.00
11.00
11.00
12.00
13.00
TEMP. IN DEGREES C.
0.00
25.00
50.00
TILT IN DEG.x10
16.52 EDST

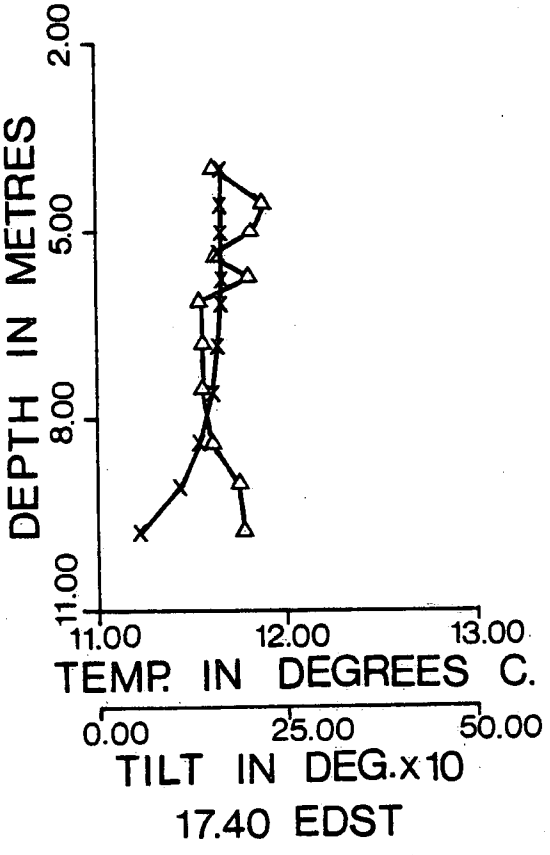
DEPTH IN METRES
2.00
5.00
8.00
11.00
11.00
12.00
13.00
TEMP. IN DEGREES C.
0.00
25.00
50.00
TILT IN DEG.x10
17.40 EDST

FIGURE 25

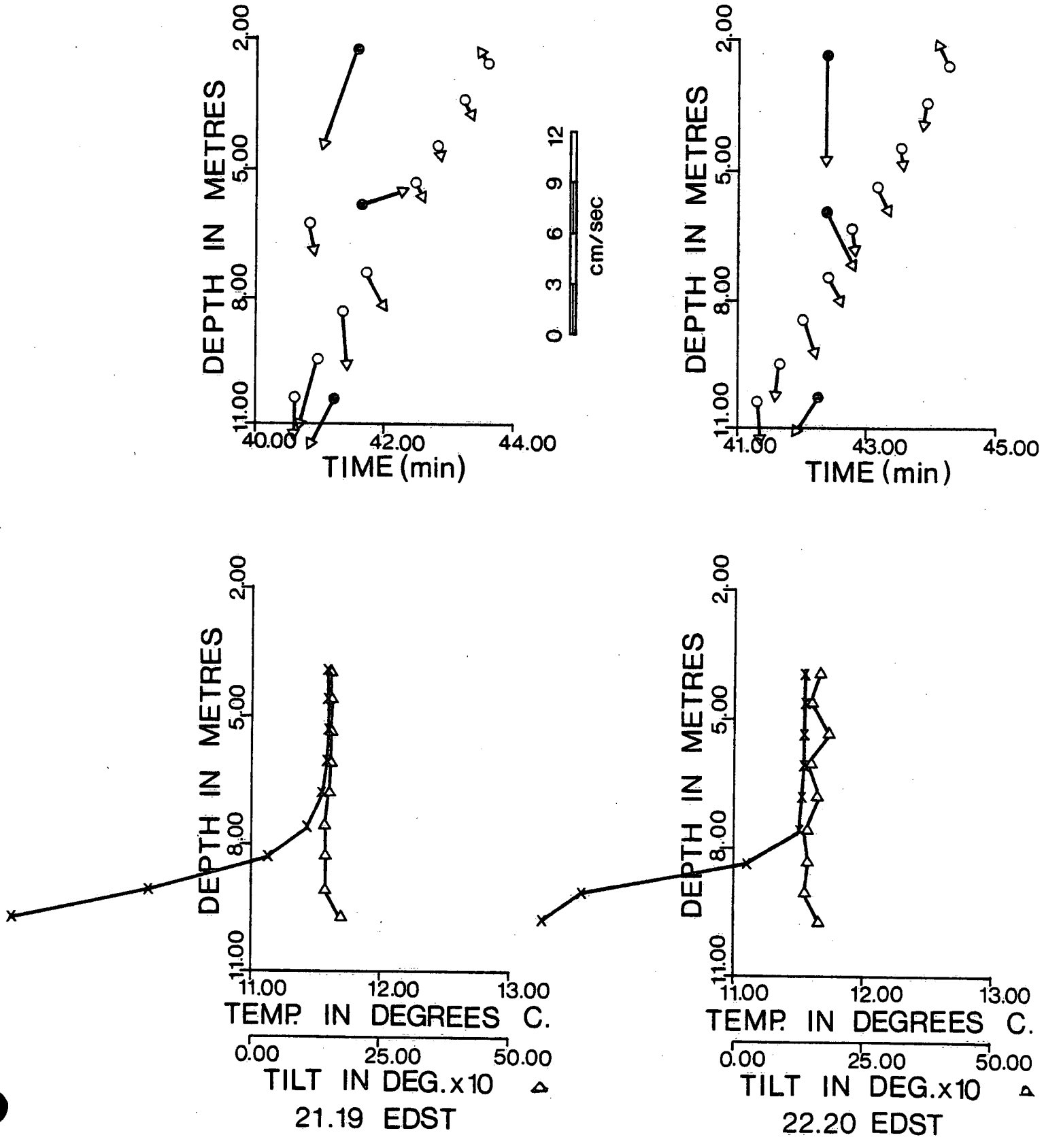
DEPTH IN METRES
2.00
5.00
8.00
11.00
40.00
42.00
44.00
TIME (min)
0
3
6
9
12
cm/sec
DEPTH IN METRES
2.00
5.00
8.00
11.00
41.00
43.00
45.00
TIME (min)
DEPTH IN METRES
2.00
5.00
8.00
11.00
11.00
12.00
13.00
TEMP. IN DEGREES C.
0.00
25.00
50.00
TILT IN DEG.x10
21.19 EDST
DEPTH IN METRES
2.00
5.00
8.00
11.00
11.00
12.00
13.00
TEMP. IN DEGREES C.
0.00
25.00
50.00
TILT IN DEG.x10
22.20 EDST

FIGURE 26

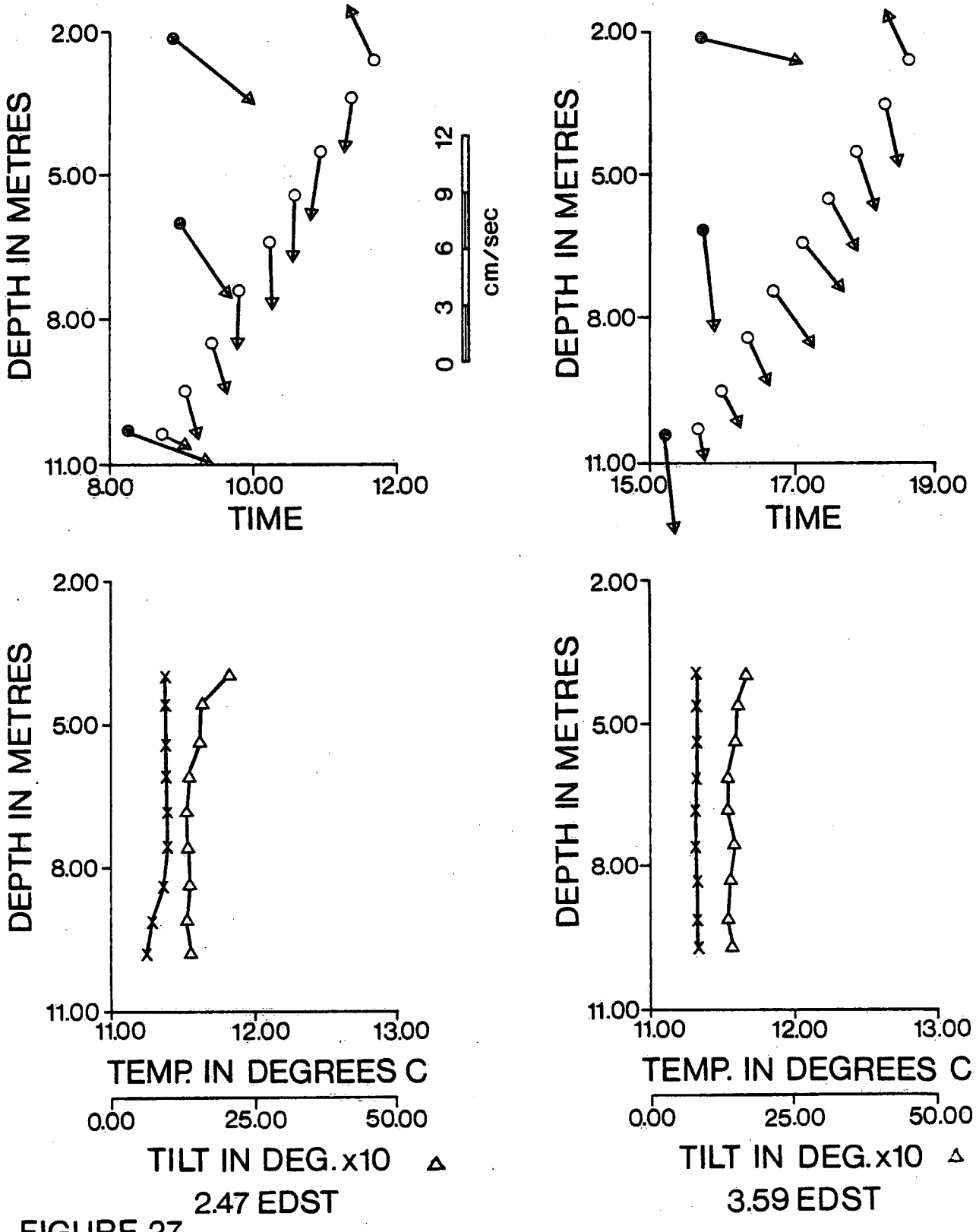
DEPTH IN METRES
2.00
5.00
8.00
11.00
8.00
10.00
12.00
TIME
0
3
6
9
12
cm/sec
DEPTH IN METRES
2.00
5.00
8.00
11.00
15.00
17.00
19.00
TIME
DEPTH IN METRES
2.00
5.00
8.00
11.00
11.00
12.00
13.00
TEMP. IN DEGREES C
0.00
25.00
50.00
TILT IN DEG. x10
2.47 EDST
DEPTH IN METRES
2.00
5.00
8.00
11.00
11.00
12.00
13.00
TEMP. IN DEGREES C
0.00
25.00
50.00
TILT IN DEG. x10
3.59 EDST

FIGURE 27

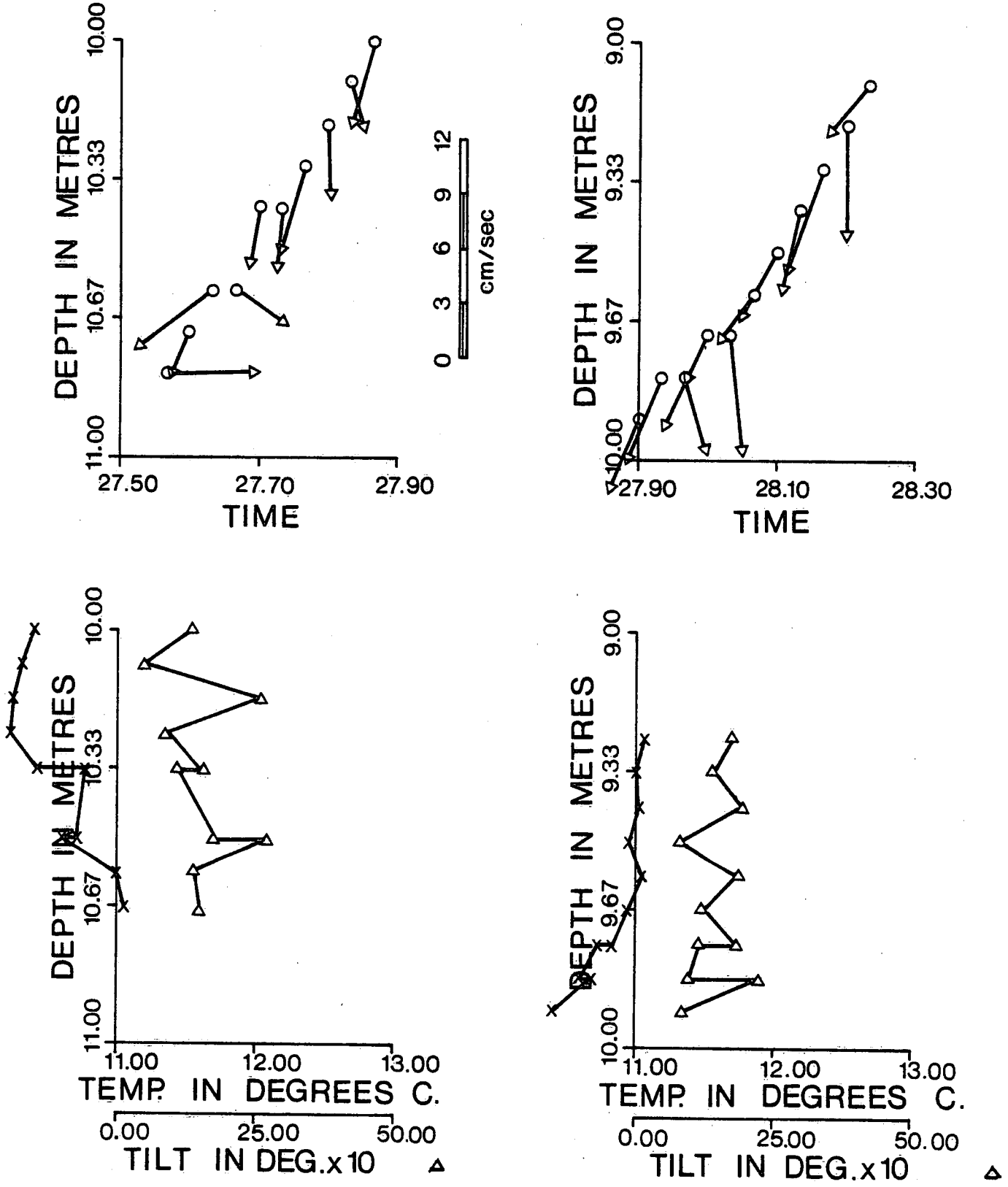
DEPTH IN METRES
10.00
10.33
10.67
11.00
27.50
27.70
27.90
TIME
0 3 6 9 12
cm/sec
DEPTH IN METRES
9.00
9.33
9.67
10.00
27.90
28.10
28.30
TIME
DEPTH IN METRES
10.00
10.33
10.67
11.00
11.00
12.00
13.00
TEMP. IN DEGREES C.
0.00
25.00
50.00
TILT IN DEG.x10
DEPTH IN METRES
9.00
9.33
9.67
10.00
11.00
12.00
13.00
TEMP. IN DEGREES C.
0.00
25.00
50.00
TILT IN DEG.x10

FIGURE 28

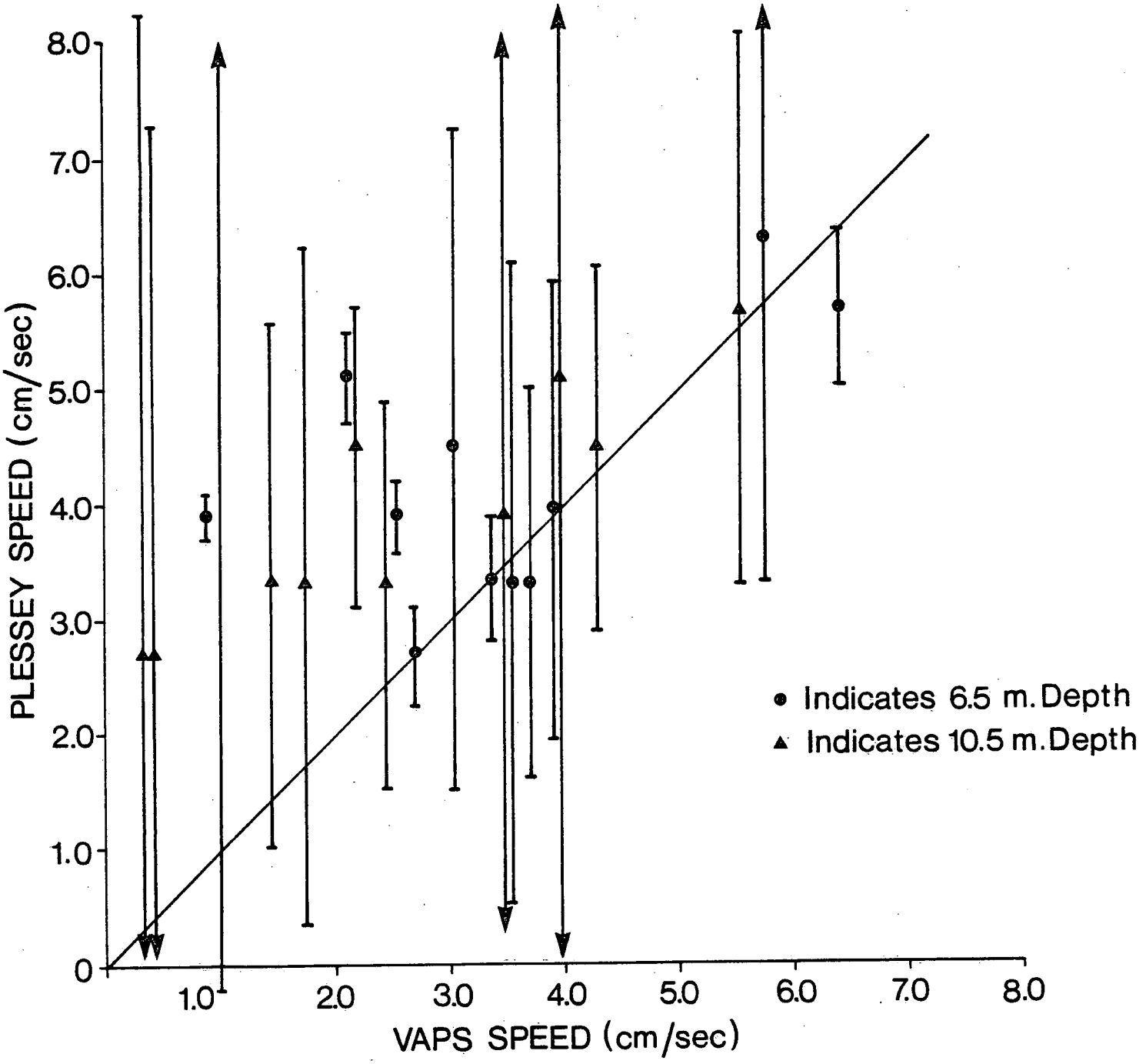

FIGURE 29. PLESSEY SPEEDS VS. VAPS SPEEDS

Time	Date	Depth	Orbital Wave Speed	Plessey		VAPS	
				Speed	Direction	Speed	Direction
6:20	9	2.5 m	26.33	10.2	101	2.04	45
5:19	9		20.80	8.0	76	5.39	156
15.45	8		17.09	6.9	221	0.9	0.0
16:52	8		16.4	4.5	190	0.88	0.0
17:40	8		16.1	4.5	168	2.63	0.0
17:59	8		14.58	4.5	193	0.49	327
3:54	9		13.0	3.3	104	3.54	327
22:20	8		11.5	6.9	182	1.72	327
2:47	9		11.2	4.5	129	3.78	327
1:40	9	2.5 m	10.20	2.1	106	4.21	327
6:20	9	6.5 m	8.88	5.1	172	3.98	126
15:45	8		7.21	3.9	250	3.5	271
17:40	8		6.9	6.6	77	1.01	293
17:59	8		5.58	2.7	166	0.38	242
20:06	8		4.59	2.7	70	0.44	166
5:00	9		3.42	5.7	126	5.56	140
21:19	8		2.9	3.3	71	1.77	161
22:20	8		2.3	3.3	148	1.49	163
0:33	9		1.68	3.3	177	2.47	149
2:47	9		1.60	4.5	134	4.31	170
1:40	9	6.5 m	1.42	4.5	201	2.17	173
17:40	8	10.5 m	3.0	4.5	234	3.06	139
6:20	9		2.99	6.3	208	5.76	110
16:52	8		2.8	3.3	213	3.64	140
19:05	8		2.01	3.9	206	3.95	170
20:06	8		1.66	3.3	197	3.72	173
5:00	9		0.71	5.7	149	6.44	127
22:20	8		0.5	2.7	211	2.8	169
23:26	8		0.49	3.3	225	3.39	146
3:54	9		0.4	5.1	168	2.16	161
0:33	9		0.27	3.9	255	2.53	133
0:40	9	10.5 m	0.20	3.9	139	0.88	80

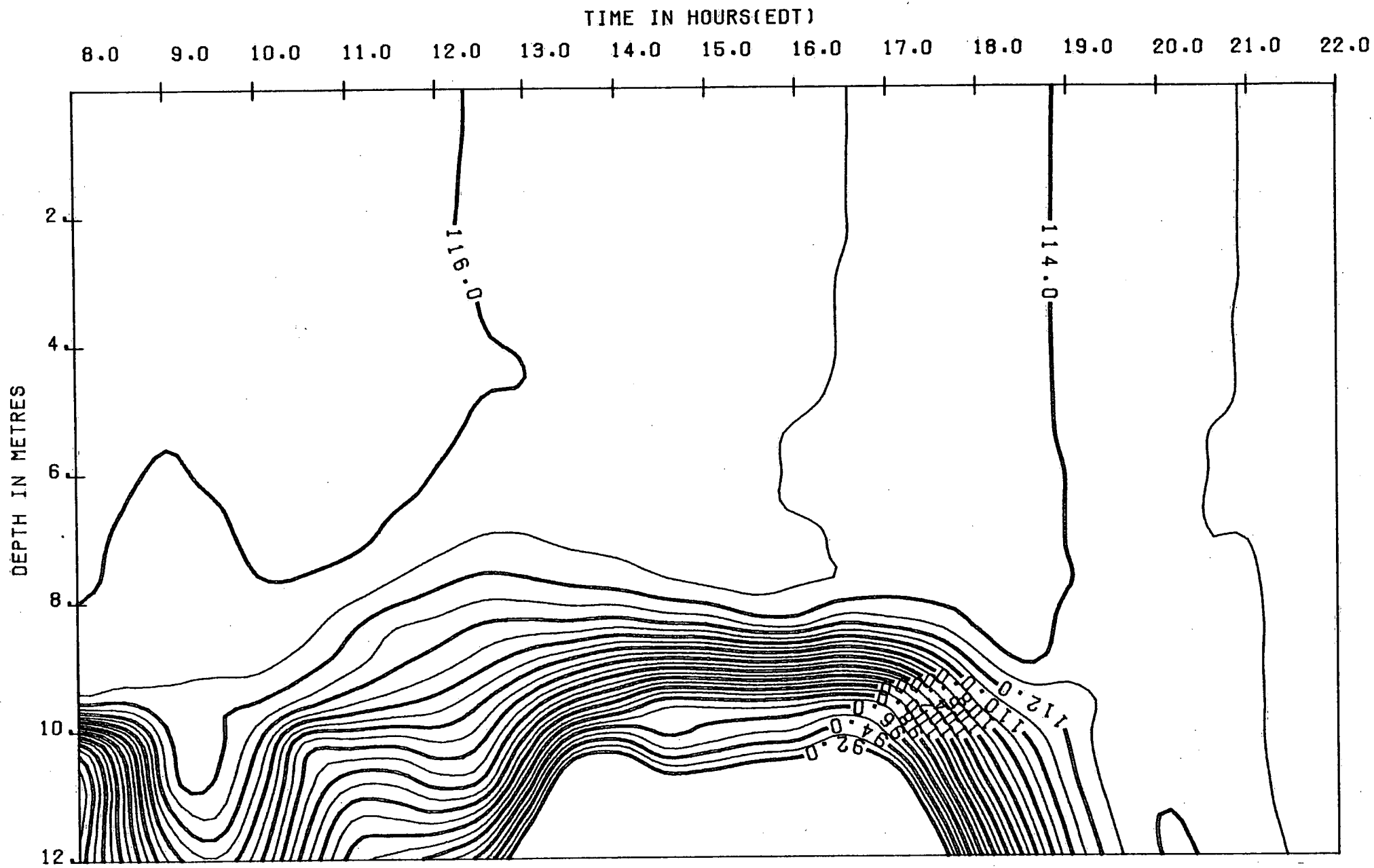

FIGURE 30 ISOTHERM OSCILLATIONS WITH DEPTH AND TIME
(SECOND FIELD TAPE - ^{o}C x 10)

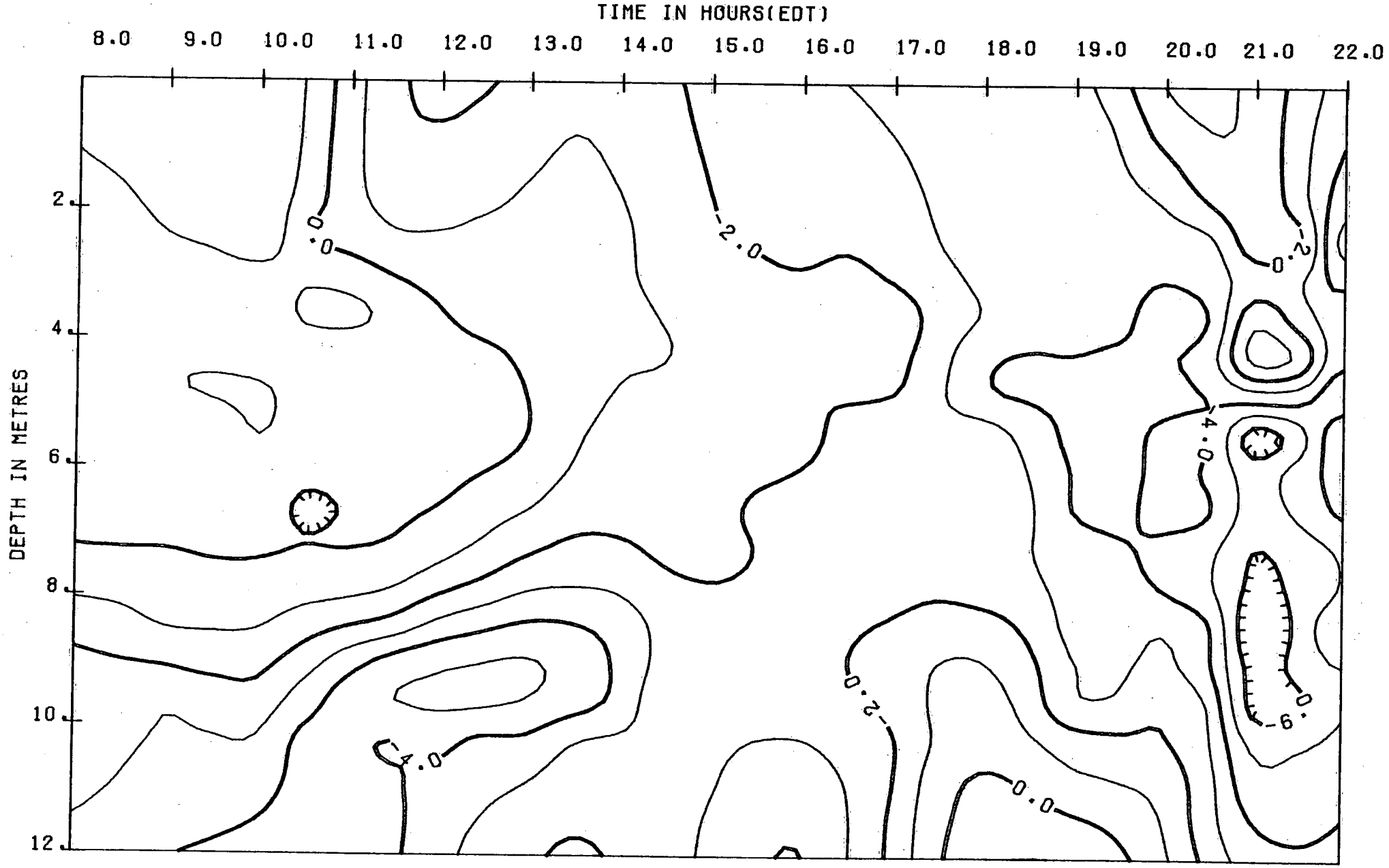

FIGURE 31 ISOPLETHS OF LONGSHORE VELOCITY COMPONENTS
(SECOND FIELD TAPE - cm/sec)

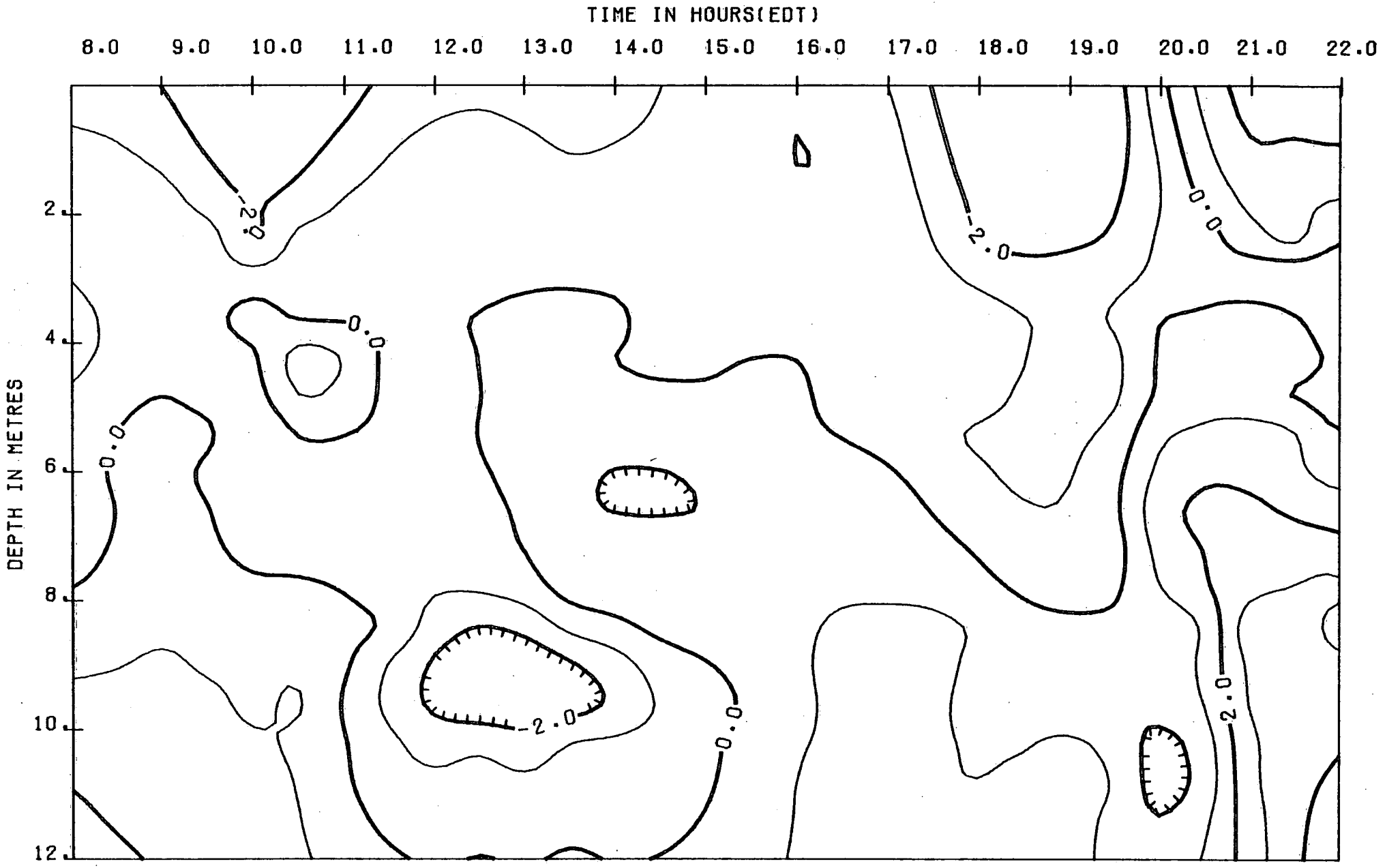

FIGURE 32 ISOPLETHS OF ON-OFFSHORE CURRENT COMPONENTS
(SECOND FIELD TAPE - cm/sec)

SUMMARY AND CONCLUSIONS

3.1 Vehicle Hull

From both the field and tow tank tests, it is apparent that there is a serious problem with the hull design. There are two components to this problem. The first is that the high drag combined with the low positive buoyancy lets the buoy travel horizontally with the wave motion which reduces the relative current between the hull and the flow field. The second problem is in the rotational motion of the hull, which was observed in the second tow tank tests, and a possible pendulum motion about its tether point. A redesign of the hull shape is presently underway.

3.2 Sensors

1) Time

Since the system failed in the middle of the tests, the length of record was not long enough to assess the accuracy of the time clock. So far there is no indication of any problems.

2) Depth

From both the field and the laboratory tests, the resolution of the depth sensor appears to be $\pm$20 cm. It is recommended that this accuracy be improved to $\pm$1 cm. It also seems that wave-induced pressure fluctuations are being recorded by the sensor, and so it is recommended that the pressure sensor have a filter installed in the circuit with a time constant of about 4 seconds.

3) Temperature

The temperature sensor seems to have worked well, although there is some evidence of a time delay in the system. This is thought to be due to the hull design and is being rectified.

4) Compass

The time constant of the compass is much too long. This is being corrected. Most of the problems with the compass may be traced to the torsional oscillations of the body, and this too is being corrected.

5) Tilt

This has been a most useful sensor for design purposes. The relatively low variation in tilt amplitude indicates that the body is vertically stable. However, it must be kept in mind that even very small

fluctuations in vertical tilt can induce fairly large current errors.

6) Speed

The speed sensor problems seem to be almost entirely caused by the problems with the hull design. Because the apparent flow vector will not be horizontal while the VAPS is profiling, off-axis response tests are necessary. There is a large deviation of speed at low speeds (less than 5 cm/s) in the profiling mode.

3.3 Data Processing

An outstanding difficulty in evaluating the data from the VAPS has been the long delay and intricate handling necessitated by the lack of an in-house capability to translate the magnetic tapes from the data logger.

Short-term measures have proved useful for a small subset of the total data collected. A number of data display and handling routines have been successfully implemented. However, an in-house capability to translate the data logger tapes is necessary. In addition, further work must be done to adapt software to the peculiar requirements of the VAPS data set.

APPENDIX A:

SENSOR CALIBRATION DIAGRAMS

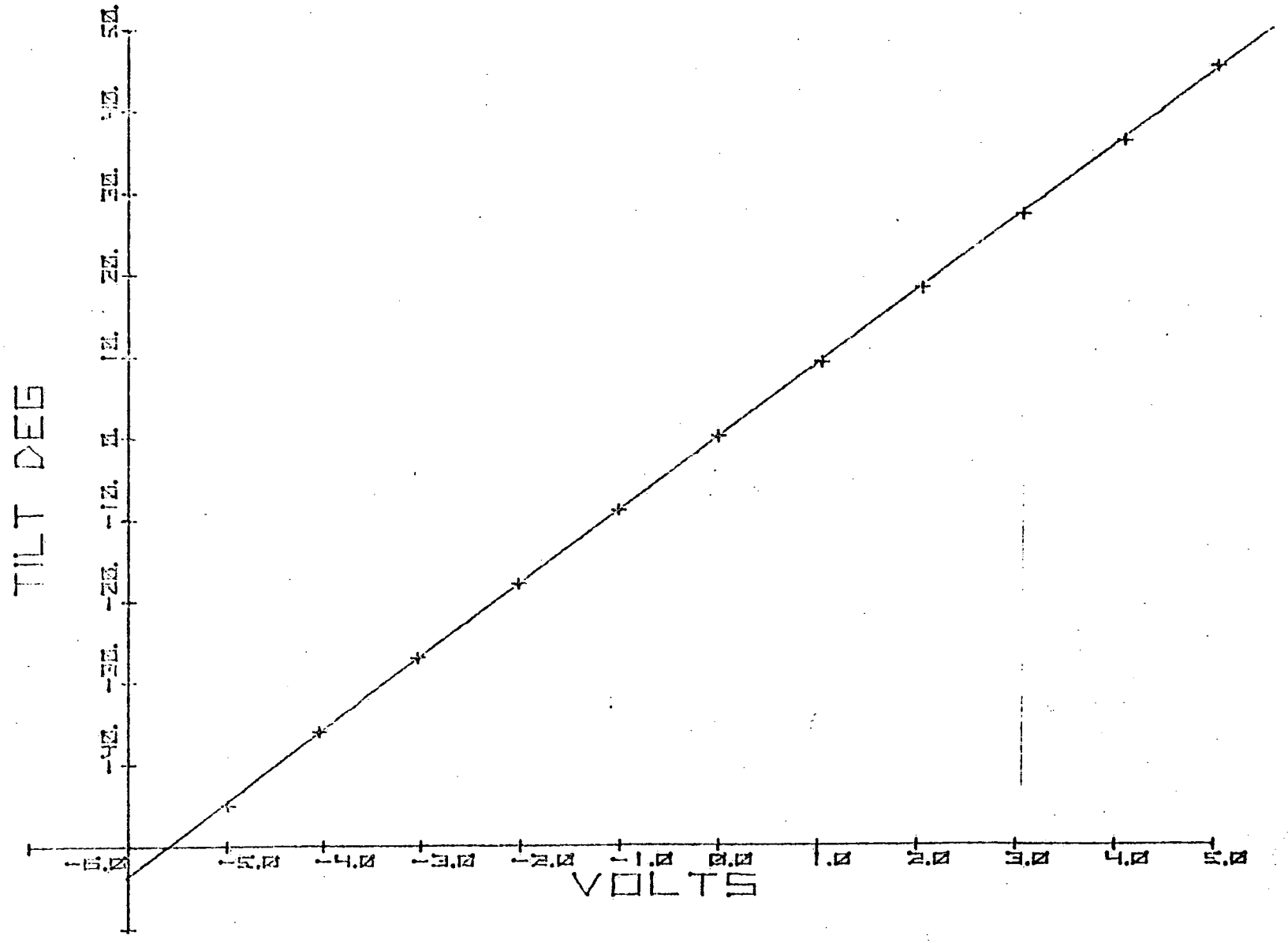

X-AXIS TRANSFER FUNCTION

HUMPHREY TILT SENSOR MODEL VI[illegible]-0402-1

S/N[illegible]

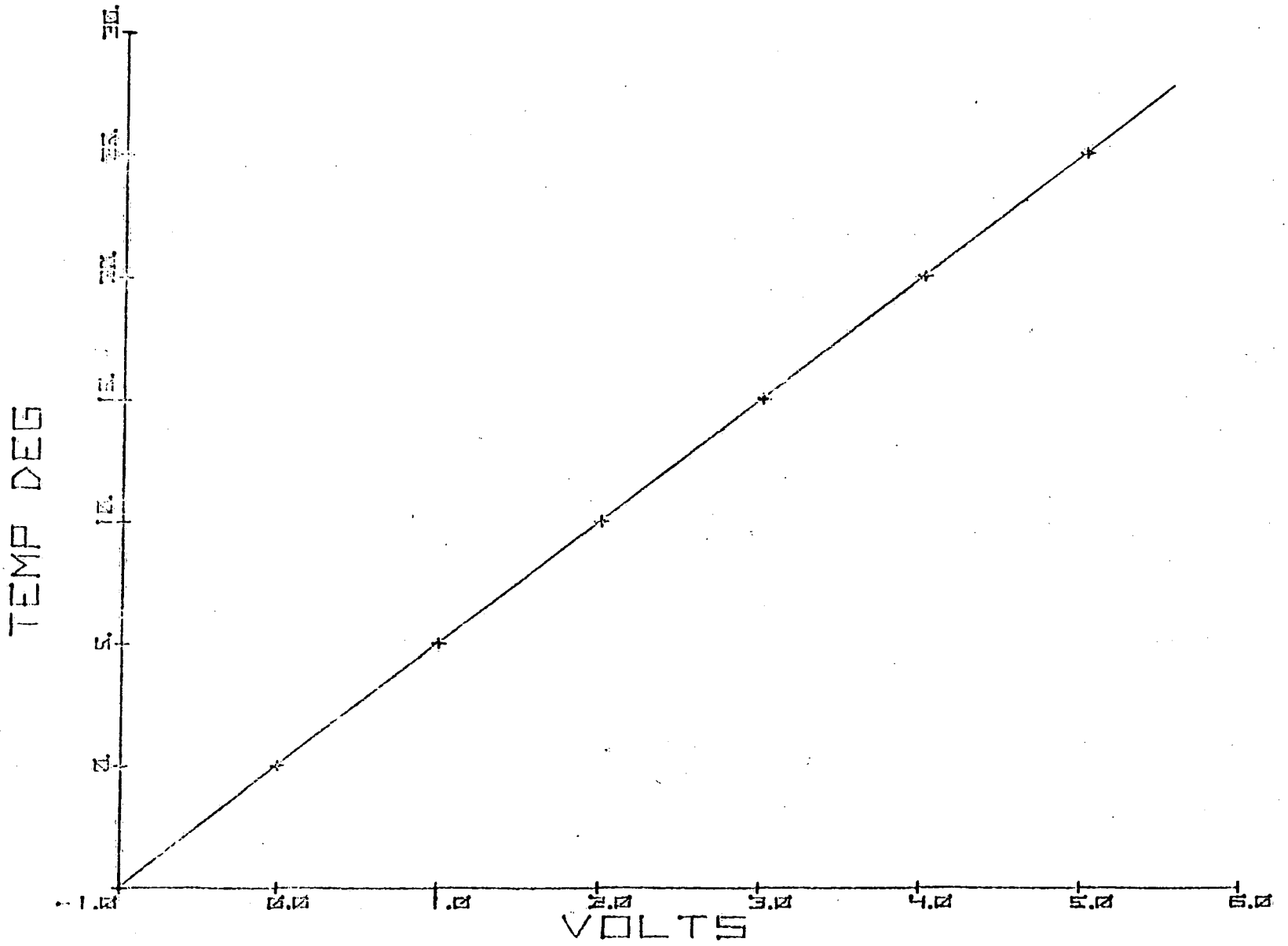

TEMPERATURE SENSOR TRANSFER FUNCTION

ROSEMOUNT MODEL 171ED S/N 9161

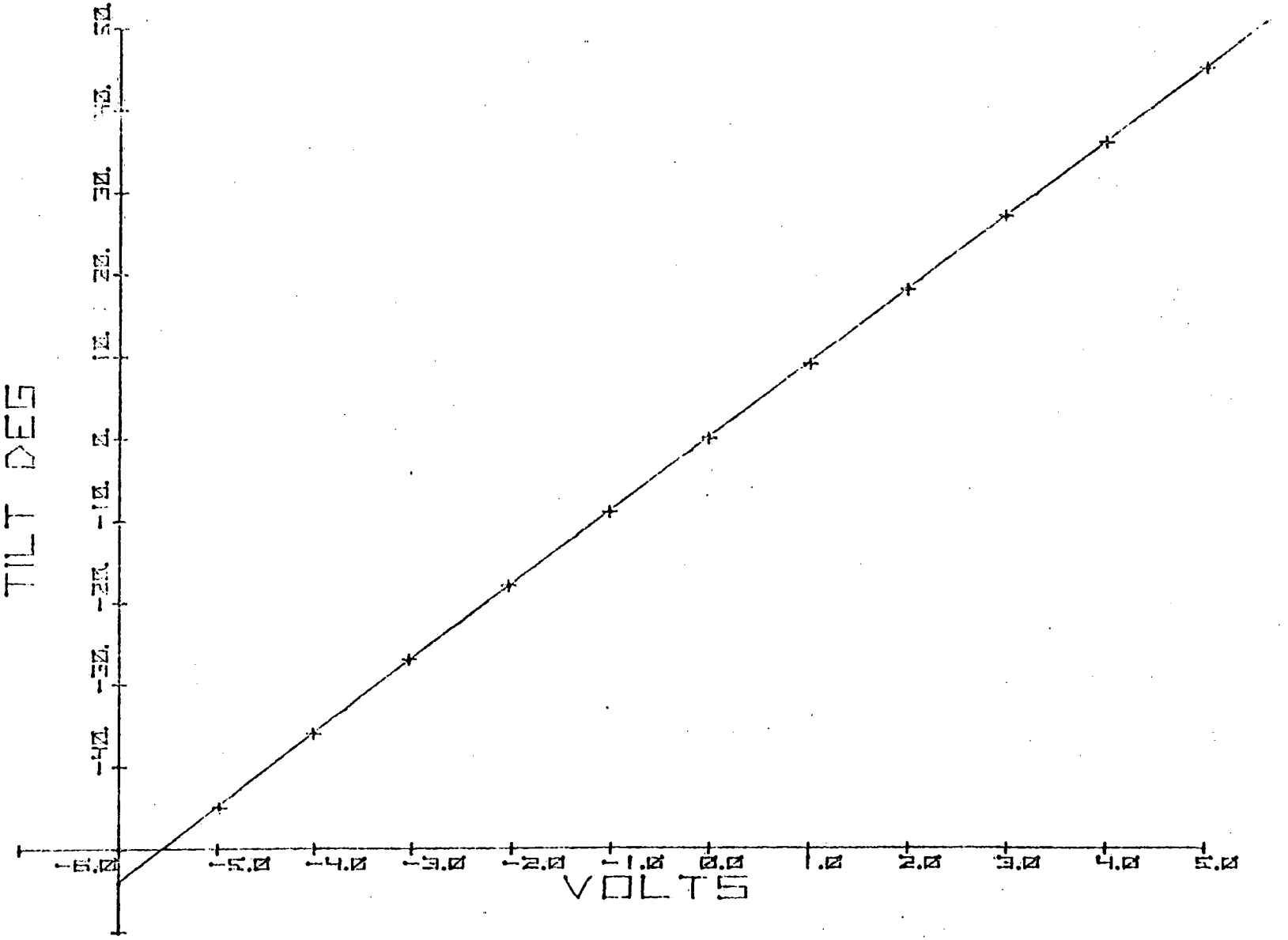

Y-AXIS TRANSFER FUNCTION

HUMPHREY TILT SENSOR MODEL VI18-0402-1

S/N

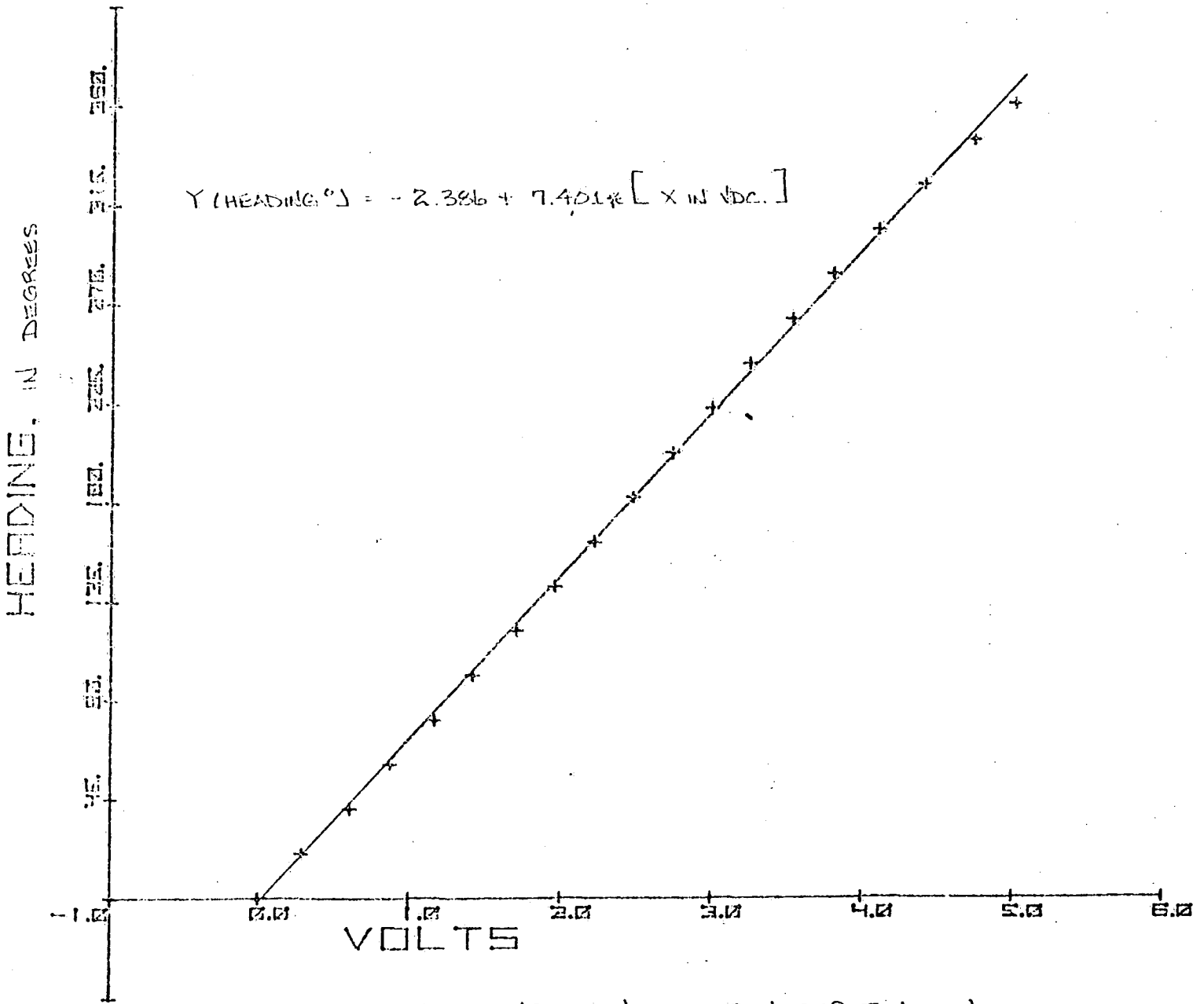

HEADING SENSOR TRANSFER FUNCTION

DIGICOURSE MODEL 101 S/N L61520

24 AUGUST 1976

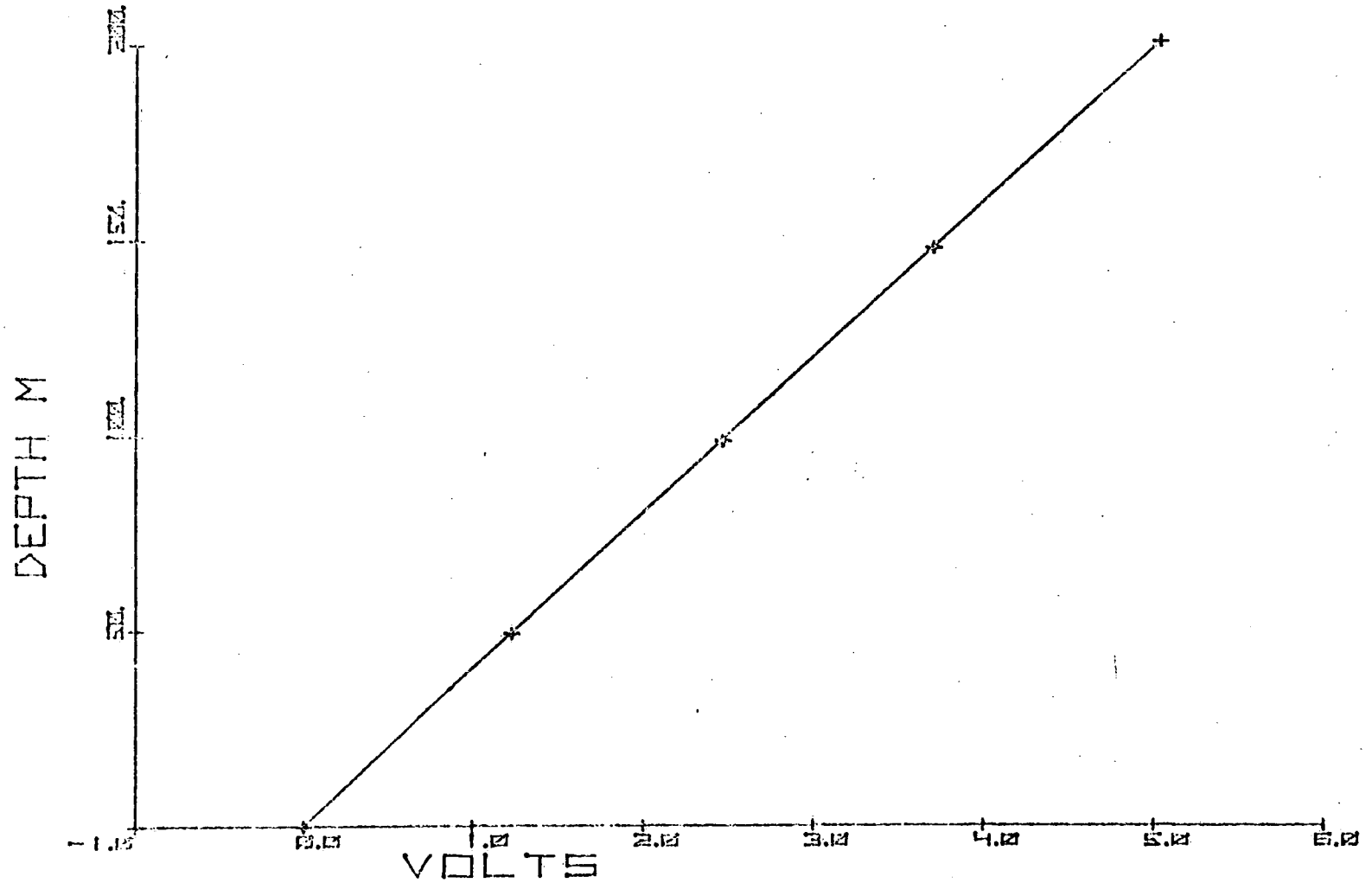
DEPTH M
VOLTS
0.0
1.0
2.0
3.0
4.0
5.0
6.0